PEOPLE'S DEMOCRATIC REPUBLIC OF ALGERIA

Ministry of Higher Education and Scientific Research

University of Amar Telidji - Laghouat

Faculty of Technology

Department of Electronics

MASTER THESIS

DOMAIN: Science & Technology

FIELD: Electronics

SPECIALTY: Instrumentation

TOUHAMI Oussama & BENMEHIRIS Makhlouf

Theme

Study and simulation of PV Emulator based on DC-DC Push-Pull Converter

Jury members:

ABOUCHABANA Nabil	Prof	President
AMEUR khaled	MCB	Examiner
HADJ AISSA Aboubakeur	MCA	Supervisor
BENMILOUD Mohammed	MCB	Co-Supervisor

2022 / 2023

Abstract

The aim of this master project is to model and study about the photovoltaic emulator (PVE), the letter is based on DC-DC push-pull converter controlled by PI controller. The PVE is designed in order to simulate the behaviour of photovoltaic panels. To achieve the objective of this master's project, we started by studying and modeling of the PV panel by its equivalent electrical circuit, then modeling and analysis of the push-pull converter through the state space representation then the average model calculation in order to define the PI parameters through frequency analysis (Bode diagram). The founded results show the effectiveness of our proposed PVE structure (DC-DC push pull converter controlled by PI).

key words: PVE: Photovoltaic emulator , DC-DC: direct current converter , PI : propotionel integral controller.

ملخص

الهدف من هذه الاطروحة هو نمذجة ودراسة المحاكي الكهروضوئي (PVE) ، بحيث تستند الاطروحة على محول الدفع والسحب DC-DC (push-pull) الذي يتم التحكم فيه بواسطة وحدة تحكم PI.
تم تصميم PVE من أجل محاكات سلوك الألواح الكهروضوئية. لتحقيق هذا المشروع، بدأنا بدراسة ونمذجة اللوحة الكهروضوئية من خلال دائرتها الكهربائية المكافئة ، ثم نمذجة وتحليل محول الدفع والسحب من خلال تمثيل فضاء الحالة ثم حساب النموذج المتوسط من أجل تحديد معلمات PI من خلال تحليل التردد (مخطط Bode). تظهر النتائج الأساسية فعالية هيكل PVE المقترح (محول سحب الدفع DC-DC المتحكم بواسطة PI).

Résumé

L'objectif de ce projet de master est de modéliser et d'étudier un émulateur photovoltaïque (EPV) basé sur un convertisseur push-pull à courant continu (CC) contrôlé par un régulateur PI. L'EPV est conçu pour simuler le comportement des panneaux photovoltaïques. Pour atteindre l'objectif de ce projet de master, nous avons commencé par étudier et modéliser le panneau photovoltaïque à travers son circuit électrique équivalent, puis nous avons procédé à la modélisation et à l'analyse du convertisseur push-pull en utilisant la représentation d'etat, suivie du calcul du modèle moyen afin de définir les paramètres PI par le biais d'une analyse fréquentielle (diagramme de Bode). Les résultats obtenus démontrent l'efficacité de notre structure d'EPV proposée.

Acknowledgements

We would like to express our heartfelt appreciation to our advisor, Prof. HADJ AISSA Aboubakeur, and our co-supervisor, Mohammed BENMILOUD, for their invaluable guidance, patience, and encouragement throughout our journey as their students. Their unwavering support and prompt responsiveness to our questions have been instrumental in our progress.

We would also like to thank the committee members, Dr.ABOUCHABANA Nabil, Dr.AMEUR khaled for serving us as our committee members. We would especially like to thank everyone helps us to get this work accomplished.

We would also like to thank our families. Words cannot express how grateful we are to our parents for all of the sacrifices that they have made. Their prayers and support for us were what sustained us thus far. We would also like to thank all of our friends who supported us in preparing this project, and incented us to strive towards our goal. Finally, I would like to thank the teaching team and administrative body of the Faculty of technology for the richness and quality of their teaching, and they go to great lengths to provide their students with up-to-date training.

TOUHAMI oussama & BENMEHIRIS makhlouf
Laghouat University
June 2023

List of Figures

Contents

Abbreviation

Abbreviation	**Definition**
C	Capacitor
d	Duty Cycle
DC	Direct current
f	Maximum Switching Frequency
G	Solar irradiance
GPV	Photovoltaic Generator
Gm	Gain Margin
Isc	Short Circuit Current
IMP	Current at Maximum Power
Ki	Integral gain of PI regulator
Kp	Proportional gain of PI regulator
L	Inductor
MPPT	Maximum Power Point Tracking
Np, Ns	Number of Cells in Parallel, Number of Cells in Series
Pm	Phase Margin
Pmax	Maximum Power
PWM	Pulse Width Modulation
PV	Photovoltaic
PVE	Photovoltaic Emulator
STC	Standard Test Condition
VMP	Voltage at Maximum Power
Voc	Open Circuit Voltage

General Introduction

Nowadays, our planet can be destroyed by burning the hydrocarbons from fossil energy for human needs. So, it is time to replace this energy with one that is suitable, renewable, whose natural renewal is fast enough to be considered as inexhaustible. Concerning, renewable and clean energies, solar energy, despite a very rapid development for the last years, still relatively marginal at the global level, far behind wind energy, biomass and especially hydraulic energy. Photovoltaic solar energy comes from the direct transformation of part of the solar radiation into electrical energy. This energy conversion is carried out through a photovoltaic cell (PV) based on a physical phenomenon called photovoltaic effect which consists in producing an electromotive force when the surface of this cell is exposed to light. The voltage generated may vary depending on the material used for the manufacture of the cell. The combination of several PV cells in series / parallel gives rise to a photovoltaic generator (GPV) which has a non-linear current-voltage characteristic (I-V) having a peak power point. The I-V characteristic of the GPV depends on the level of Irradiance and the temperature of the cell as well as the aging of the whole. In addition, its operating point depends directly on the load that it feeds. [1]

PV emulators play a crucial role in various applications, such as solar power system design, optimization, and performance evaluation. They allow engineers, researchers, and technicians to analyze and study the behavior of PV systems under different operating conditions, without relying on actual sunlight or physical PV modules. This flexibility enables extensive testing and analysis in a controlled and repeatable environment.

The main purpose of PV emulators is to replicate the electrical characteristics and output of solar panels. Solar panels generate direct current (DC) electricity when exposed to sunlight, and their output is influenced by factors like irradiance levels, temperature, shading, and

other environmental conditions. PV emulators simulate these characteristics by producing programmable DC voltage and current outputs, which can be adjusted to mimic the behavior of specific PV modules or arrays.

Based on ref generally PV emulators divided on three disciplines, power electronics that main a structure of DC-DC converter [2], a PV model[3] and control strategy used for the PV emulator.The hybrid-mode controlled method [4][5][6] and the resistance comparison method [7][8] produce a stable output for the PV emulator at any load condition. Much research has been conducted on the PV emulator. However, there are no specific papers that compile and discuss about the PVE based on push pull converter.

The main objective of this manuscript is to study and simulation of the PV emulator system that consists of the PV model based electrical circuit, the control strategy based PI controller, and the power converter based on DC-DC Push-pull. This project is structured around three chapters organized as follows:

- **The first chapter** provides a comprehensive overview of photovoltaic (PV) generators, focusing on the concepts of PV emulation and DC-DC converter topologies. It explores the fundamental components involved in DC-DC converters, which play a crucial role in PV systems. The chapter begins by introducing the significance of PV generator and the increasing need for accurate PV emulator. It discusses the challenges faced in PV system testing and highlights the importance of PV emulators as essential tools for evaluating the performance of various PV systems under different conditions. Furthermore, the chapter explores various topologies of DC-DC converters utilized in PV systems.

- **The second chapter** This chapter focuses on the modeling and control of push-pull converter using a state space representation approach, along with the design and analysis of a PI controller based on Bode diagrams. The chapter begins by presenting an overview of the push-pull converter operation, highlighting its advantages and applications. The converter fundamental principles, including the operation modes and switching mechanisms, are explained to provide a solid foundation for the subsequent discussions.

  Next, the design and analysis of a PI controller for the push-pull converter are discussed. The Bode diagram technique is employed to determine the appropriate controller parameters, taking into account the desired closed-loop performance specifications. The

analysis involves assessing the stability, steady-state error, and bandwidth of the controlled system, ensuring robust and efficient operation.

- **Finally, the third chapter** provides a functional description of a photovoltaic (PV) emulator, along with the mathematical modeling of a PV panel using a singal diode model.

  The simulation of the PV emulator performance is discussed in depth. MATLAB/Simulink, are utilized to simulate the emulator's behavior under different operating conditions.

  Furthermore, the chapter addresses the performance of the PV emulator and its validation. The emulator performance is evaluated through extensive simulations, comparing its output with the expected behavior of a real PV panel. Performance indicators such as power output, and dynamic response are analyzed to ensure the accuracy and reliability of the emulator.

Chapter 1

PV Emulators and Dc-Dc Converters

1.1 Introduction

Photovoltaic emulators replicate the behavior of PV modules and arrays by emulating their electrical characteristics. They mimic the voltage-current (V-I) curves of real PV devices, allowing researchers, manufacturers, and engineers to assess system performance under various operating conditions. Photovoltaic emulators can accurately replicate factors such as solar irradiance, temperature, shading, and environmental conditions.

The emulators provide a controllable power source (DC-DC converter) that can simulate different solar power levels and dynamics. They allow for precise control over parameters such as maximum power point tracking (MPPT), which ensures the PV system operates at its optimal operating point for maximum power extraction. Photovoltaic emulators are used for testing and optimization of PV system components, algorithm development, grid integration studies, and educational purposes. DC-DC converters, on the other hand, are power electronic devices used to manage the power flow within a PV system. They perform the crucial function of converting and controlling the voltage and current levels between different components of the system. DC-DC converters enable efficient power transfer and facilitate the integration of PV systems with the electrical grid or other energy storage systems.[2]

1.2 Photovoltaic generator

In 1839, the French physicist Alexandre E. Becquerel discovered the photovoltaic effect, which involves the conversion of solar energy into electrical energy using semiconductor materials.

A photovoltaic cell, also known as a solar cell, is typically made of high-purity silicon. It is constructed with a PN (positive-negative) junction that forms a potential barrier. When photons from sunlight strike the PN junction, they create pairs of opposite electrical charge carriers known as electron-hole pairs. These carriers are then separated due to the presence of the PN junction.

The electrons are directed towards the N-type semiconductor region, while the holes are directed towards the P-type semiconductor region. This separation of charges generates a voltage across the junction. Since the separated electrical charges are surplus carriers and have an infinite lifetime, and the voltage across the PN junction remains constant, the junction acts as a stable electric cell when exposed to light.

In summary, the photovoltaic effect allows the conversion of solar energy into electrical energy by utilizing a PN junction in a photovoltaic cell.[1]

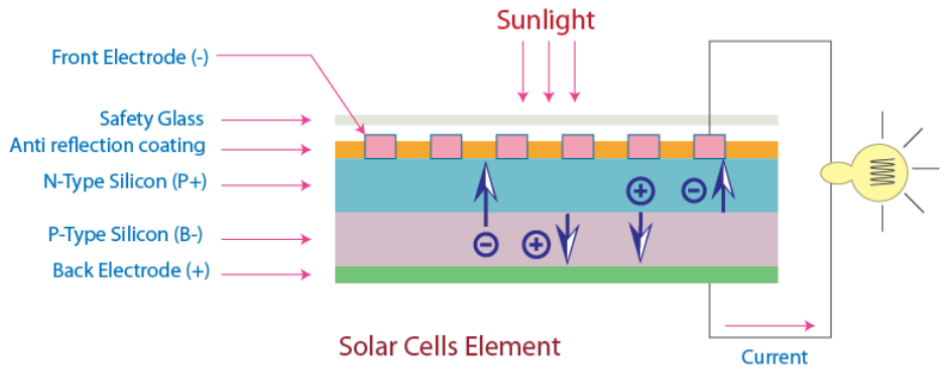

Figure 1.1: Structure of a photovoltaic cell using silicon as PV material.

1.3 Need For PV Emulator

Creating a controlled environment for testing photovoltaic (PV) equipment poses challenges as it is difficult to reproduce consistent and repeatable conditions. The electrical characteristics of a PV panel are influenced by several factors, such as the amount of irradiance it receives, the panel's temperature, and the materials used in its construction.

To overcome these challenges and enable more efficient analysis and optimization of PV systems, a PV emulator is employed. This emulator is designed to simulate the current and voltage characteristics of a photovoltaic panel under diverse conditions. By providing consistent electrical characteristics, the PV emulator allows for easier analysis and optimization of

PV systems.

By utilizing a PV emulator, researchers and engineers can study the performance of PV equipment under different scenarios, including varying levels of irradiance and temperature. This enables them to assess the impact of these factors on the system's efficiency, reliability, and overall performance.

Ultimately, the PV emulator plays a crucial role in facilitating accurate and reliable testing of PV equipment, providing a valuable tool for the development and improvement of photovoltaic systems.[9]

A huge variety of solar panels exist. It would be prohibitively expensive to purchase each type of panel and test individually. A PV emulator would be able to simulate many different types of solar panels, under various temperature and weather conditions.

1.4 Overview of photovoltaic emulator

The PV emulator system introduced by the researcher consists of three main components, as depicted in Figure 1.2.

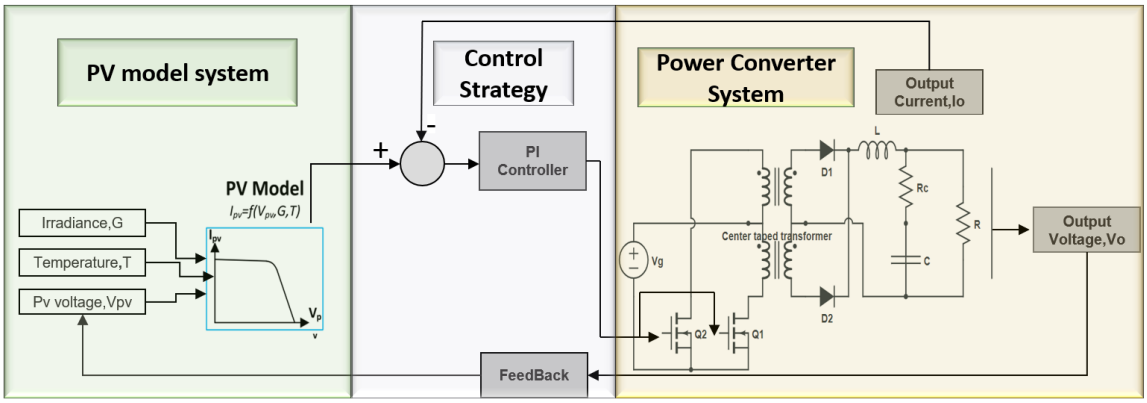

Figure 1.2: The three parts of the PV emulator system.

- The first component is the PV model, which is responsible for generating the I-V (current-voltage) characteristics of the PV module signal. This signal serves as input to the closed-loop power converter system, enabling emulation of the PV module's characteristics. The accuracy of the PV emulator heavily relies on the PV model; however, real-time calculations are essential for the proper operation of the PV emulator. Therefore, the PV model used in the PV emulator application should be simplified while maintaining accurate production of the I-V characteristics.

- The second component of the PV emulator system is the control strategy. The control strategy acts as an interface between the PV model and the closed-loop power converter system. It determines the operating point of the PV emulator by integrating the PV model with the closed-loop power converter system. An effective control strategy should accurately track the signal generated by the PV model, provide a stable output from the PV emulator, require minimal computational burden, be adaptable to different types of PV modules without necessitating a complete redesign of the control strategy, and not interfere with the closed-loop power converter system or the load [10].

- The third part of the PV emulator system is the power converter. The power converter is used to change the I-V characteristic signal produced by the PV model into the I-V characteristic capable of transmitting power. The power converter affects the dynamic perfor- mance and the efficiency of the PV emulator. The actual PV module dynamic response is approximately a 10th of a microsecond [9]. Therefore, a good PV emulator needs to have a similar dynamic response to the actual PV module.

1.5 Photovoltaic model

There are two considerations in the PV model used for the PV emulator. The first consideration is the types of PV models used, of which there are two. The models are the electrical circuit model and the interpolation model, as shown in figure 1.3.

The second consideration is the methods used to implement the PV model inside the controller of the PV emulator; there are five of these methods, which include direct calculation method, look-up table method, piece-wise linear method, neural network method, and curve segmentation method.[3]

1.5.1 Implementation of photovoltaic model

The controller incorporates the PV mathematical model to compute the reference signal for the PV emulator. However, the processor of the controller can become overburdened by the complex mathematical equations involved. Consequently, the calculation of the reference point for the PV emulator may experience delays, leading to incorrect responses to disturbances. This highlights the crucial requirement for real-time calculation of the PV model in the PV emulator.

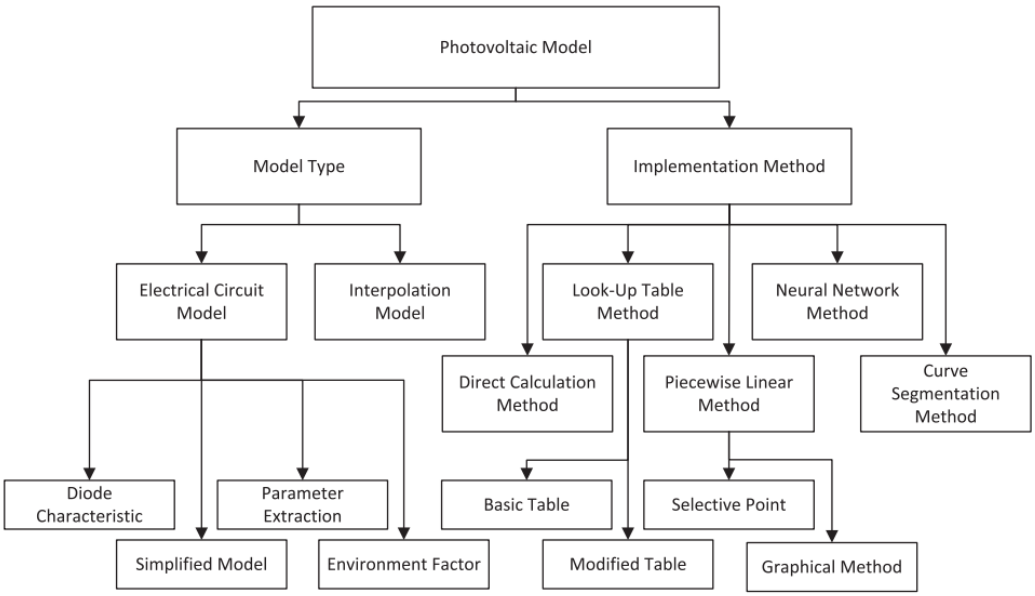

Figure 1.3: PV model overviews in the PV emulator application.

To address this challenge, an appropriate implementation method is necessary, which depends on the capabilities of the controller and the complexity of the PV model. Figure 1.4 illustrates five methods commonly used to implement the PV model into the PV emulator controller.

These methods aim to optimize the performance and computational efficiency of the PV emulator. They may involve simplifying the mathematical equations, utilizing lookup tables or approximation algorithms, employing parallel processing techniques, or using specialized hardware for faster calculations. The choice of implementation method depends on factors such as the available resources, processing capabilities, and desired accuracy of the PV emulator system.

By selecting an appropriate implementation method, the PV model can be effectively integrated into the PV emulator controller, ensuring real-time calculations and enabling accurate responses to disturbances.

1.6 Electrical circuit model

The electrical circuit model is the PV modeling represented in the form of an electrical circuit and the PV characteristic equation is derived using the Kirchhoff current law [11]. This model is also known as the analytical model and is commonly used in the photovoltaic emulator

applications [3].

1.6.1 Diode model approximation based PV emulator

The diode model approximation is one of the oldest methods used for the design of emulators. Since PV panel exhibit non-linear behavior, researchers have used the diode based approximation method to emulate solar PV characteristics. The most commonly used single diode and double diode model based approximation techniques have accurately replicated the I-V and P-V characteristics of PV panel. Hence, panels used for the design of efficient emulator in literature [3,4]. The schematic representations of single and double diode models are shown in figure 1.4 (a) and 1.4 (b).

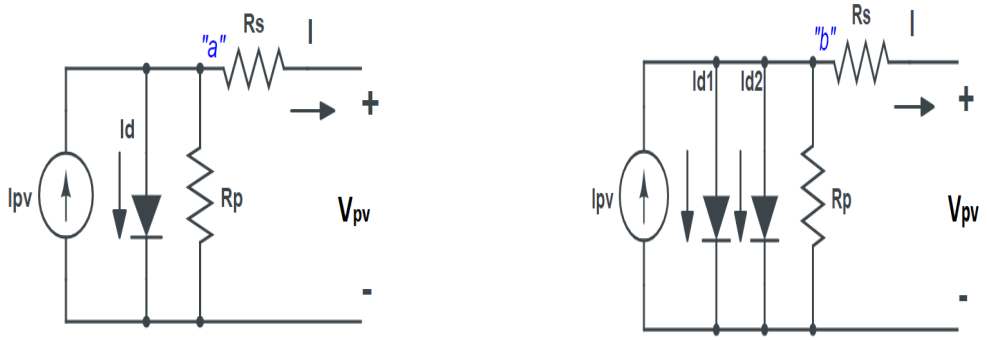

(a) (b)

Figure 1.4: (a). Single diode model, (b). Double diode model

Applying Kirchhoff's current law at node 'a' and node 'b', the output equation of single diode and double diode models are given as:

$$I = I_{pv} - I_s \left[e^{\frac{V_{pv}+IR_s}{AV_T}} - 1 \right] - \frac{V_{pv}+IR_s}{R_p} \tag{1.1}$$

$$I = I_{pv} - I_{s1} \left[e^{\frac{V_{pv}+IR_s}{A_1V_T}} - 1 \right] - I_{s2} \left[e^{\frac{V_{pv}+IR_s}{A_2V_T}} - 1 \right] - \frac{V_{pv}+IR_s}{R_p} \tag{1.2}$$

Where:

I : is the output current of the PV cell or module.

V : is the voltage across the PV cell or module.

Ipv: is the photocurrent generated by the incident light.

Is_1, Is_2: are the reverse saturation current of the diodes.

Rs: is the series resistance.

Rp : is the shunt resistance.

A_1, A_2: are the diode ideality factors.

V_t: is the thermal voltage, approximately equal to (k*T) / q where: k is the Boltzmann constant, T is the temperature in Kelvin, and q is the elementary charge.

1.6.2 Simplified model

The single diode model is simplified by removing the parasitic resistance from the equation. This type of model is called the single diode model with a series resistance or the 1D1R model [12] [13] [14], and the circuit representation is shown in Fig 1.5.

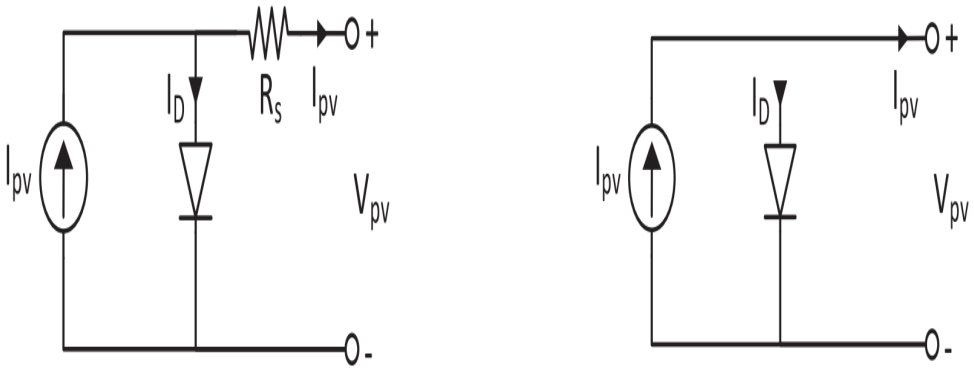

Figure 1.5: a) The single diode model with a series resistor (1D1R Model). b) The ideal Model (1D Model).

This model excludes the parallel resistance from the equation (the value of Rp in Eq. (1.1) is set to infinity). There is also the ideal model or the 1D model used in the PV emulator application. This type of model does not include the parasitic resistance, as shown in Fig.1.5(b) and the characteristic equation is shown in Eq. (1.3). This type of model is inaccurate since the series resistance highly affects the PV module output .[3]

$$I_{pv} = I_{ph} - I_s \left[e^{\frac{V_{pv}}{AV_T}} - 1 \right] \tag{1.3}$$

1.7 Parameter extraction of PV emulator

The parameter extraction, or also known as the parameter estimation, is used when the theoretical parameters such as I_{ph}, I_s, R_s, R_p, and A are unavailable[15][16]. The parameter

extraction is done by using two methods, which are by using the selected value from I-V and P-V characteristic curve of PV module or is based on an algorithm that fits the I-V characteristic graph of PV cell. The parameter extraction that uses selective points to determine the theoretical parameters requires the open circuit voltage (V_{oc}), the short circuit current (I_{sc}), the maximum power voltage (V_{mp}), and the maximum power current (Imp).Although these methods are simple, the inaccurate measurement of the selective point significantly affects the PV model accuracy . The curve fitting method uses all the data from the I-V characteristic curve to extract the theoretical parameter. This method provides a higher level of confidence in accuracy since multiple points in the I-V characteristic curve are used. However, this method requires high computational power and a large data memory. The accuracy of the theoretical parameters also depends on the fitting algorithm and criteria. Further, the curve fitting method requires experimental data from the I-V characteristic curve from the manu- facturer, which is usually not given in the datasheet. The PV module contains parasitic resistance which consists of the series resistor, Rs, and the parallel resistor, Rp. The series resistance represents power losses due to the current circulation throughout the PV module. The series resistance does not affect the open circuit voltage and only affects the short circuit current. The increase in series resistance results in the decrease of the short circuit current and reduces the slope of the I-V characteristic curve of the PV module in the constant voltage region. A more accurate calculation of the series resistor is obtained using the curve fitting algorithm; however, there is an equation to calculate series resistor based on the selective point as shown in Eq (1.4).

The parallel resistor represents the leakage current at the p-n junction. It does not affect the short circuit current and only affects the open circuit voltage. The increase in parallel resistance results in the decrease of the open circuit voltage and the increase in the slope of the I-V characteristic curve of the PV module in the constant current region. If the slope at the short circuit current in the I-V characteristic curve is almost zero, the parallel resistance is assumed as infinity[17].

$$R_s = \frac{V_{mp} + \frac{I_{mp}(V_{oc}-V_{mp})}{(I_{sc}-I_{mp})In\left(1-\frac{I_{mp}}{I_{sc}}\right)}}{I_{mp} + \frac{{I_{mp}}^2}{(I_{sc}-I_{mp})In\left(1-\frac{I_{mp}}{I_{sc}}\right)}} \tag{1.4}$$

The ideality factor is another component considered when using the PV electrical circuit model. It is also known as the diode quality factor or the n-factor. In an ideal condition, the ideality factor is equal to one. However, in practice, this value varies depending on the non-

ideality in the junction behavior. The ideality factor varies from one to two depending on the fabrication process used .Itisclosetoone when the diode is dominated by the recombination in the quasi-neutral region and it is close to two when the PV module is dominated by the recombination in the depletion region[3].

1.8 Environment factor

The PV panel manufacturer commonly provides the parameter at the Standard Test Condition (STC) where the solar irradiance at STC, Gref, is 1000 W/m2 and temperature at STC, Tref, is 298 K or 25 °C. For nominal operating cell temperature, NOCT (K), the parameter is determined at an irradiance of 800 W/m2 and temperature of 20 °C.[18] The parameter extraction only produces the constant value of photo-generated current at a given V_{oc}, I_{sc}, V_{mp} and I mp. This value is manipulated according to solar irradiances and the temperature of the PV module. The PV module temperature affects the I-V PV characteristics. As the temperature increases, the short circuit current increases, open circuit voltage decreases, and maximum power decreases.[17] [19].

The photo-generated current, Iph, is directly proportional to the sun's irradiance, G (W/m2). The relationship between Iph and G is shown in Eq. (1.5).[20]

$$I_{ph}(G,T) = \frac{G}{G_{ref}} \left[I_{ph(ref)} + K_{Ti} \left(T - T_{ref} \right) \right] \tag{1.5}$$

where Iph(ref) is the photo-generated current at the STC, KTi is the temperature coefficient of the short circuit current (A/°C), which is commonly provided by the manufacturer , T is the temperature of the PV module (°C), and Tref is the module temperature at the STC. The saturation current, Is, is also affected by the environment. However, Is is only affected by the module temperature and it is not affected by the irradiance. Is is calculated using Eq. (1.6). However, a more simplified saturation current equation is used in the PV emulator application.[20][18]

$$I_s(T) = I_{s(ref)} \left(\frac{T}{T_{ref}} \right)^3 \exp \left[\frac{qE_g}{Ak} \left(\frac{1}{T_{ref}} - \frac{1}{T} \right) \right] \tag{1.6}$$

where Is(ref) is the saturation current at the STC, q is electron charge (1.6 × 10–19 C), k is Boltzmann's constant (1.38 × 10–13 J/K), and Eg is the thermal gap (eV). There are also other terms called the thermal voltage, VT, and the thermal gap which are affected by

the environment in the PV electrical circuit model. The thermal voltage increases as the temperature increases and it this is represented in Eq. (1.7). The thermal gap, Eg is 1.12 eV for the crystalline silicon PV panel and 1.75 eV for the amorphous silicon PV panel[3].

$$V_T = \frac{kT}{q} \tag{1.7}$$

1.9 DC-DC Converters

DC/DC converters are electronic devices that are designed to convert a DC voltage level to another level of DC voltage. These devices are widely used in various electronic devices and applications to regulate the voltage level required for proper operation. DC/DC converters are classified based on their topology, mode of operation, and output voltage regulation. The topology of the DC/DC converter determines the switching method used to regulate the voltage level. The mode of operation refers to how the converter operates during the switching process. The output voltage regulation refers to the method used to regulate the output voltage of the converter. The most common types of DC/DC converters are the Buck Converter, Boost Converter, Buck-Boost Converter, Flyback Converter, and Forward Converter,and push-pull converter.

The mode of operation of the DC/DC converter can be classified into two types: continuous mode and discontinuous mode. In continuous mode, the current flows continuously through the inductor or transformer, whereas, in discontinuous mode, the current flows only during a part of the switching cycle. The output voltage regulation of the DC/DC converter can be achieved through different methods such as feedback control, and peak current control. Feedback control is the most commonly used method for regulating the output voltage of the DC/DC converter.[2][21]

1.10 Topologies of DC-DC Converter

The topologies of DC-DC converter are designed to meet specific demand of DC loads. There are several types of DC-DC converter that can be functioned as switching mode regulators that can regulate the unregulated DC voltage with conversion to suitable utilization voltage through increase or decrease the value of DC output voltage by using power switching devices for PWM switching at a fixed frequency which are buck, boost, buck-boost, cuk, Single Ended

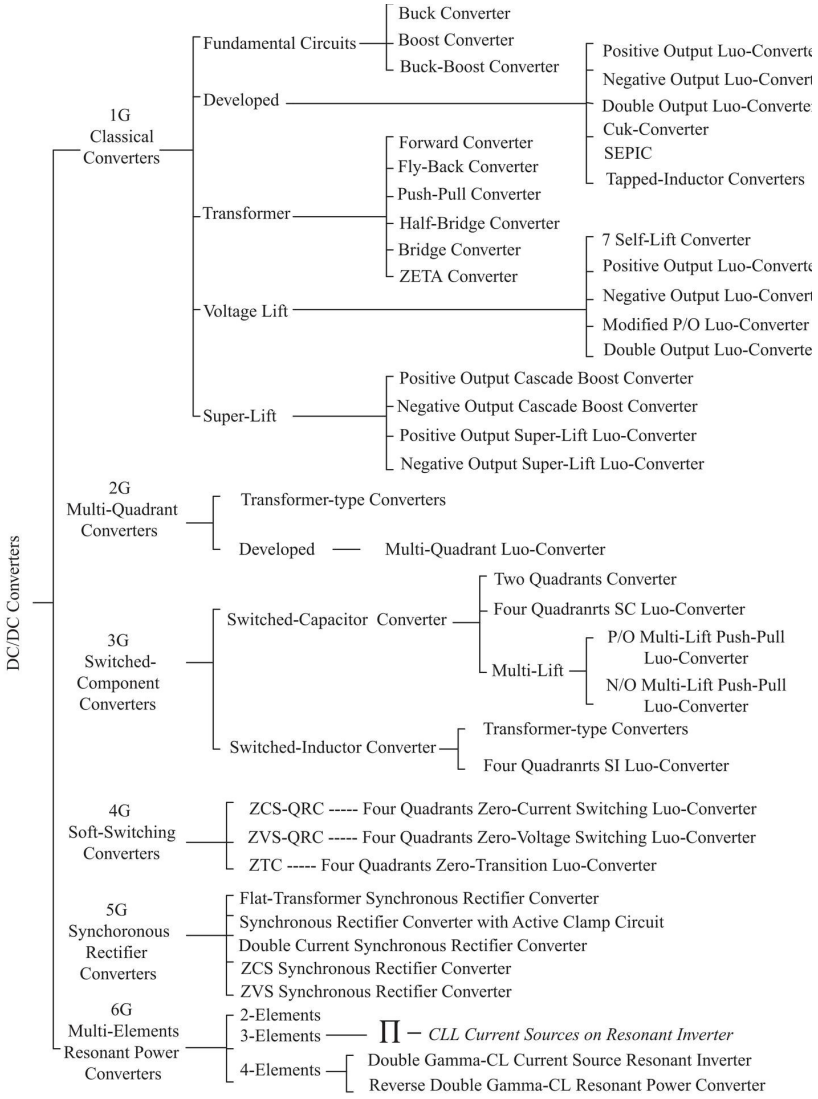

Figure 1.6: DC-DC Converter Family.

Primary Inductor Converter (SEPIC) and flyback–boost converter. Each converter requires the power switching devices for turn-on and turn-off when it is needed. The power switching devices such as MOSFETs, IGBTs, BJTs and thyristors are used depending upon the applications and parameters of designing the circuit. In order to trigger the power switching devices, appropriate gate drive signals by using gate driver circuit should be considered. The DC-DC converters are driven by Pulse Width Modulation (PWM) switching to control the converter voltage.[22].

1.10.1 Isolated Converters

Isolated converters provide electrical isolation between the input and output circuits, typically using transformers or optocouplers. The primary advantage of isolated converters is the ability to provide galvanic isolation, which means there is no direct electrical connection between the input and output. This isolation offers several benefits, including safety, noise reduction, and the ability to handle voltage differences and eliminate ground loops. Isolated converters are commonly used in applications where safety and isolation are critical, such as medical equipment, industrial controls, power supplies, and communication systems.[23]

Examples of isolated converter topologies include the flyback converter, forward converter, push-pull converter, and full-bridge converter.

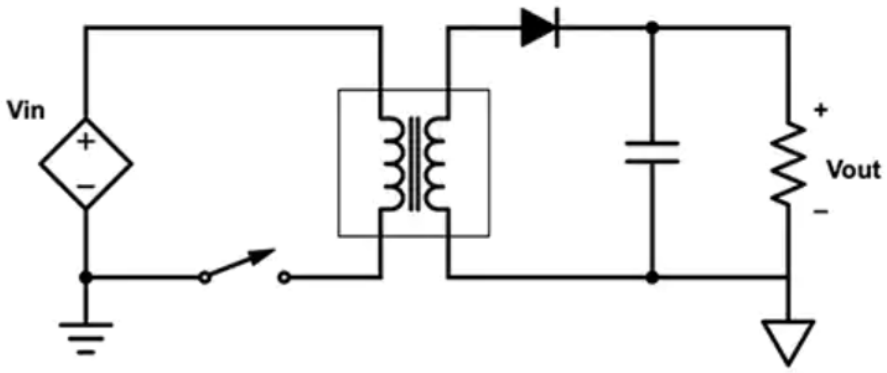

Figure 1.7: Typical isolated circuit diagram.

1.10.2 Non-Isolated Converters

Non-isolated converters, as the name suggests, do not provide electrical isolation between the input and output circuits. The input and output share the same reference ground, and there is a direct electrical connection between them. Non-isolated converters are typically simpler and more cost-effective compared to isolated converters. They are commonly used in applications where isolation is not necessary or where the input and output share the same ground reference.

Examples of non-isolated converter topologies include the buck converter, boost converter, buck-boost converter, and SEPIC (Single-Ended Primary Inductor Converter). The choice between isolated and non-isolated converters depends on the specific requirements of the application. Isolated converters are preferred when electrical isolation is necessary

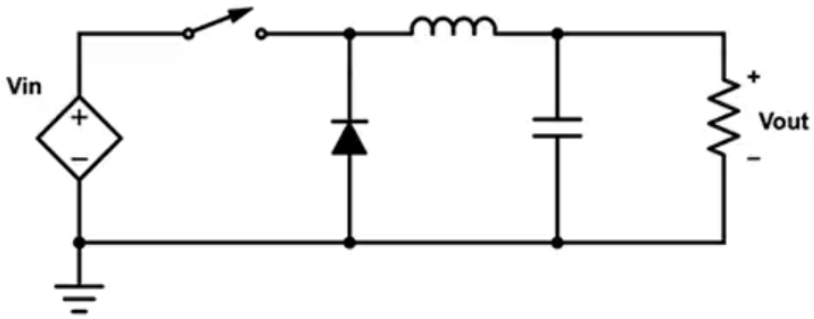

Figure 1.8: Typical Non-isolated circuit diagram.

to ensure safety, minimize noise, or handle voltage differences. Non-isolated converters are typically used in applications where isolation is not required, and cost and simplicity are important factors. It's important to consider the specific requirements, safety considerations, and standards applicable to the application when selecting between isolated and non-isolated converters.[23]

1.11 Fundamental Components of DC-DC

1.11.1 Power Switch

The power switch in a DC-DC converter controls the flow of current through the converter. It can be a transistor, such as a MOSFET or BJT, or an insulated gate bipolar transistor (IGBT). The switch is typically operated in a switching mode (on or off) to regulate the output voltage. The switching action is controlled by a pulse-width modulation (PWM) signal.[24] [25]

1.11.2 Inductance (L)

Inductors are used in DC-DC converters to store and release energy. They help smooth out the current flow and can be used in combination with capacitors to create a low-pass filter. The inductance value affects the converter's performance.[26] [27]

1.11.3 Capacitance (C)

Capacitors are employed in DC-DC converters to store and supply energy. They help reduce voltage ripple and stabilize the output voltage. Capacitors can be used in conjunc-

tion with inductors to form a low-pass filter. The capacitance value affects the converter's performance.[28] [29]

1.11.4 Diodes

Diodes are used in certain types of DC-DC converters for rectification purposes. They allow current to flow in only one direction and prevent reverse flow. Diodes are typically employed in buck-boost converters and flyback converters.

The behavior of a diode can be described by the following equation:

$$I_D = I_S \left(e^{\frac{V_D}{nV_T}} - 1 \right)$$

Where: I_D is the diode current, I_S is the reverse saturation current, V_D is the voltage across the diode, n is the ideality factor, and V_T is the thermal voltage ($V_T = \frac{kT}{q}$, where k is Boltzmann's constant, T is the temperature in Kelvin, and q is the charge of an electron).

1.12 Conclusion

In conclusion, the chapter on PV emulators and DC-DC converters provided an overview of important concepts and definitions in this field. The chapter emphasized the significance of PV emulators for simulating photovoltaic systems and assessing their performance. Various DC-DC converter topologies were discussed, highlighting their suitability for different applications. Overall, the chapter established the need for PV emulators in system testing and development, contributing to the advancement of renewable energy technologies.

Chapter 2

Modeling and control of the Push-Pull Converter

2.1 Introduction

The push-pull converter is a popular topology used in DC-DC power conversion applications. It is a type of switching converter that provides an efficient means of stepping up or stepping down voltage levels while maintaining isolation between the input and output.

The push-pull converter consists of a transformer, two switches (usually MOSFETs or transistors), and a diode bridge. The transformer is the key component that enables voltage conversion and isolation. It typically has a center-tapped primary winding and two secondary windings.

In this chapter, we will present the mathematical model of the push-pull converter (1.2 kW, 36–375 V) by modeling, analysis and its control through PI controller.

2.2 Push-pull Converter

The circuit diagram of the converter is as in Fig 2.1. It consists of two active switches (Q1 and Q2), two diodes (DI and D2), center tapped transformer (N1:N2 turns ratio) and passive elements capacitor (C) and inductor (L). The input voltage is (vg), output voltage is v(t), R is load resistance, and (Rc) is equivalent series resistance of the capacitor, two forward converters are operating back to back in push pull converter.

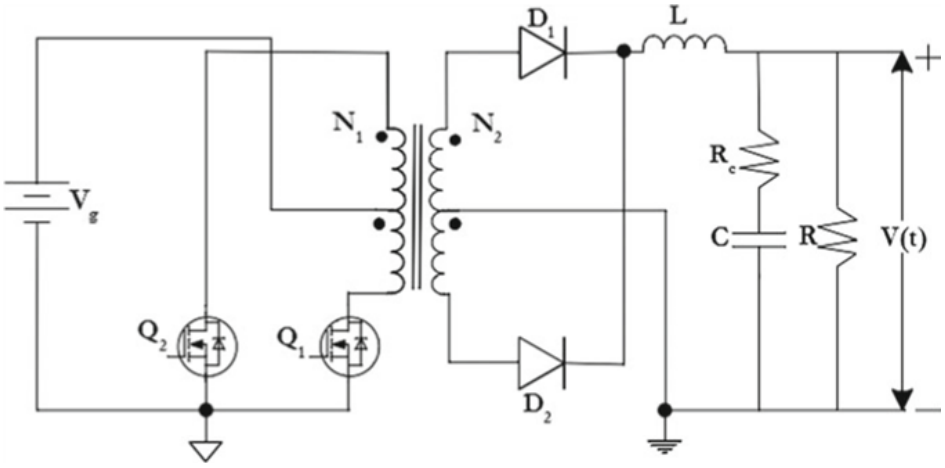

Figure 2.1: Circuit diagram of push–pull converter.

2.3 Operation of push-pull Converter

During one half of the cycle, one forward converter is operating to transfer power to the load, and during the second half of the cycle, the second forward converter is operating to transfer power to the load [30].

2.3.1 When Q1 is ON and Q2 is OFF

In this mode Vg , A2 and Q1 form the primary of the converter. Due to magnetic coupling, the polarity at the dot end is positive, and as a result, diode D1 is forward biased and D2 is reverse biased. The active secondary winding B1 and D1 delivers power to the load through the inductor and capacitor as shown in Fig 2.2 [30].

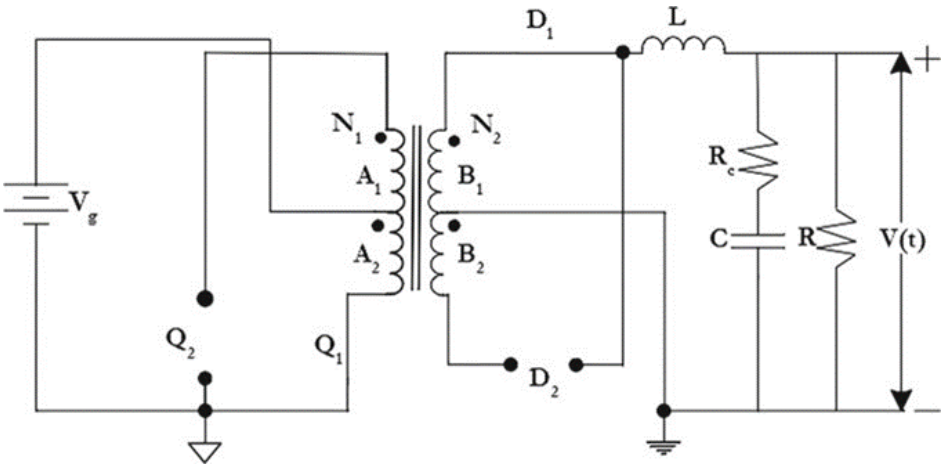

Figure 2.2: Circuit diagram When Q1 is ON and Q2 is OFF

2.3.2 When Q2 is ON and Q1 is OFF

In this mode Vg, A1 and Q2 form the primary of the converter. The polarity at the dot end is negative, and as a result, diode D2 is forward biased and D1 is reverse biased. Through the active secondary winding B2 and D2 power is transferred to the load through the inductor and capacitor as shown in Fig 2.3 [30].

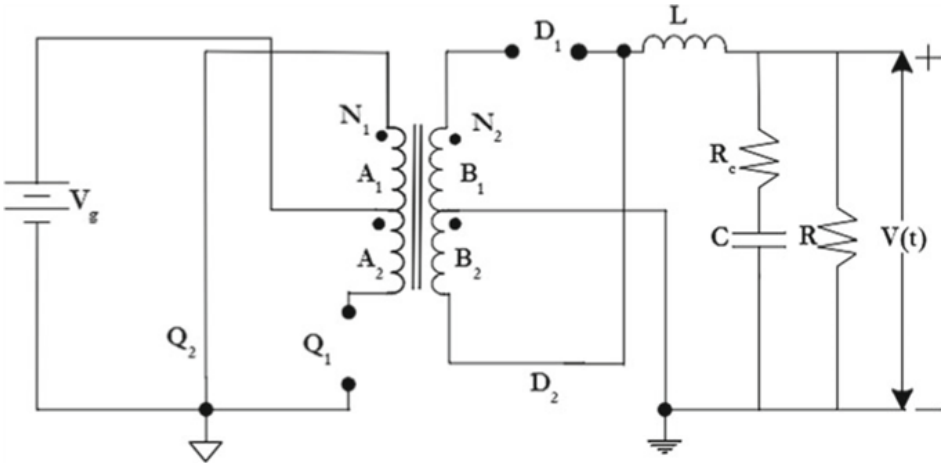

Figure 2.3: Circuit diagram When Q2 is ON and Q1 is OFF

2.3.3 When Both Q1 and Q2 are OFF

When both the primary switches are OFF, there is no transfer of power from primary to secondary. In the secondary, the inductor freewheels the current by sharing current through diodes D1 and D2 as in Fig 2.4. The voltage across all the transformer winding is zero [30].

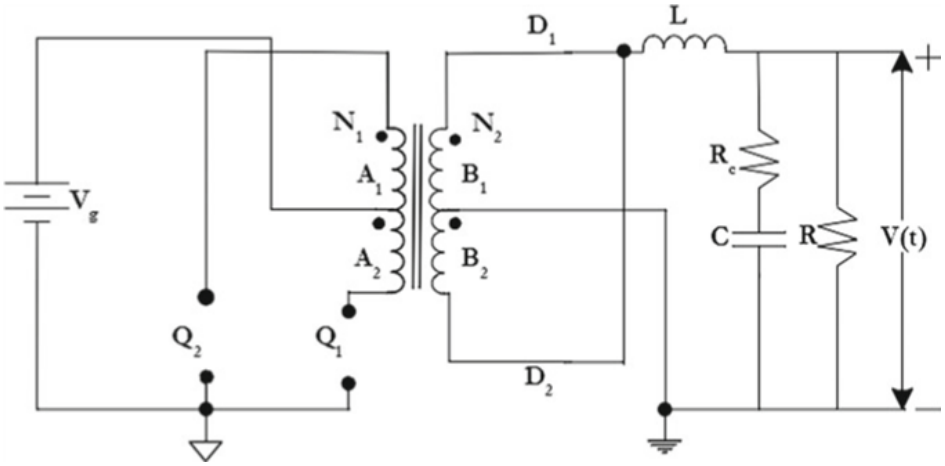

Figure 2.4: When Both Q1 and Q2 are OFF

For our work we used the following specification represented by the following tables 2.1 and 2.2:

1	**Description**	**Value**
2	Power output	1.2 kW
3	Output voltage	375 V
4	Switching frequency	100 kHz
5	Maximum duty cycle	0.45
6	Converter efficiency (assumed)	90%

Table 2.1: The specification of the Converter.

S. no	Component/parameter	Formula	Value
1	Input power	$P_{\text{in}} = \frac{P_{\text{out}}}{0.9}$	1.33 kW
2	Maximum average input current	$I_{\text{in}} = \frac{P_{\text{in}}}{V_{\text{in}}}$	33.33 A
3	Transformer turns ratio	$N = \frac{V_{\text{out}}}{2 \times D_{\min} X V_{\text{in}}}$	12
4	Maximum average output current	$I_{\text{out}} = \frac{P_{\text{out}}}{V_{\text{out}}}$	3.2 A
5	Filter inductor value	$L \geq \left(\frac{N_2}{N_1} V_{\text{in}} - V_{\text{out}} \right) \frac{t_{\text{on}}}{\Delta I}$	570 mH
6	Output filter capacitor	$C = \frac{1}{8} \frac{\Delta I}{\Delta V} T$	1.6uF

Table 2.2: Component/parameter values

Where ΔI and ΔV are current and voltage ripple, respectively

$$\Delta I = \frac{Vin \times \Delta T}{2 \times L \times f} \tag{2.1}$$

$$\Delta V = \frac{\Delta IL \times (D \times Ton) \times (1 - D)}{2 \times C} \tag{2.2}$$

2.4 Modeling apraoch of The Push-pull converter

In this chapter, state space averaging technique is used to model the push–pull converter to obtain the transfer functions of the converter. In this technique, the dynamic model of the converter is represented by equations of the form:

$$\begin{aligned} K\dot{x} &= Ax + Bu \\ y &= Cx + Eu \end{aligned} \tag{2.3}$$

A is state matrix, B is input matrix, C is output matrix, E is direct transition matrix, and x and y are input and output vector, respectively. The above equations are state and output

equation of the model. The current flowing through the inductor I_L and voltage across the capacitor (V_C) is taken as state variables. The output voltage (V) and output current (I) are considered as output variables. The two distinct modes of operation in the converter for the purpose of modeling are:

• Mode 1: When one of the primary switches Q1 or Q2 is turned ON, the transfer of energy from primary to secondary circuit takes place and inductor current increases.

• Mode 2: When both primary switches are turned off and energy stored in the inductor freewheels through secondary diodes. A push–pull converter consisting of switches, diodes, parasitic elements, inductor and capacitor is considered for modeling the converter. The equivalent series resistance of the capacitor R_C is considered when modeling the converter.

The inclusion of parasitic elements along with their loss components results in a precise model with improved system performance.

Mode 1: (Q1 is ON, Q2 is OFF)

For the duration dTs, the equivalent circuit of the converter is as in Fig 2.5

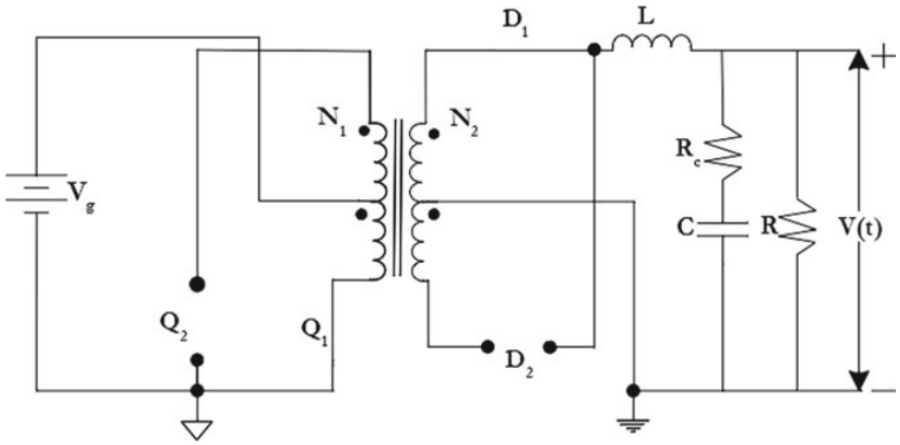

Figure 2.5: Equivalent circuit when one switch is conducting

Applying Kirchhoff's law at the dot across the inductance we find:

$$V_L + V_R = V_{N_2} \tag{2.4}$$

$$V_L = L\frac{di}{dt} \text{ and } V_R = Ri_R \tag{2.5}$$

$$i_R = i_L - i_c \tag{2.6}$$

$$i_c = \frac{Ri_L}{Z_c + R_c + R} \tag{2.7}$$

$$Z_c i_c + (R_c + R)i_c = Ri_L \text{ and } Z_c i_c = V_c \tag{2.8}$$

$$V_c + (R + R_c)i_c = Ri_L \tag{2.9}$$

$$i_c = \frac{Ri_L}{R + R_c} - \frac{V_c}{R + R_c} \tag{2.10}$$

$$V_c = \frac{1}{c}\int i_c dt \Rightarrow i_c = c\frac{dV_c}{dt} \tag{2.11}$$

$$c\frac{dV_c}{dt} = \frac{Ri_L}{R + R_c} - \frac{V_c}{R + R_c} \tag{2.12}$$

Based on equation (2.6) :

$$i_R = i_L - \frac{Ri_L}{R + R_c} + \frac{V_c}{R + R} \tag{2.13}$$

$$i_R = \frac{(R + R_c)i_L - Ri_L}{R + R_c} + \frac{V_c}{R + R_c} \tag{2.14}$$

$$i_R = \frac{R_c i_L}{R + R_c} + \frac{V_c}{R + R_c} \tag{2.15}$$

$$V = Ri_R = \frac{RR_c}{R + R_c}i_L + \frac{R}{R + R_c}V_c \tag{2.16}$$

Based on equation (2.4) :

$$V_L = V_{N_2} - V, \quad with \quad V = V_R \tag{2.17}$$

$$V_{N_2} = \frac{N_2}{N_1}V_{N_1} \tag{2.18}$$

$$V_{N_1} = V_g \tag{2.19}$$

$$L\frac{dI_L}{dt} = \frac{N_2}{N_1}V_g - \frac{RV_c}{R + R_c} - \frac{RR_c I_L}{R + R_c} \tag{2.20}$$

$$i_L = \frac{N_1}{N_2}i_g \tag{2.21}$$

The state equation and output equation are:

$$\begin{bmatrix} L & 0 \\ 0 & C \end{bmatrix} \begin{bmatrix} \frac{\mathrm{d}i_\mathrm{L}}{\mathrm{d}t} \\ \frac{\mathrm{d}v_\mathrm{c}}{\mathrm{d}t} \end{bmatrix} = \begin{bmatrix} -\frac{RR_\mathrm{c}}{R+R_\mathrm{c}} & -\frac{R}{R+R_\mathrm{c}} \\ \frac{R}{R+R_\mathrm{c}} & -\frac{1}{R+R_\mathrm{c}} \end{bmatrix} \begin{bmatrix} i_\mathrm{L} \\ v_\mathrm{c} \end{bmatrix} + \begin{bmatrix} \frac{N_2}{N_1} \\ 0 \end{bmatrix} v_g \tag{2.22}$$

$$\begin{bmatrix} v \\ i_\mathrm{g} \end{bmatrix} = \begin{bmatrix} \frac{RR_\mathrm{c}}{R+R_\mathrm{C}} & \frac{R}{R+R_\mathrm{C}} \\ \frac{N_2}{N_1} & 0 \end{bmatrix} \begin{bmatrix} i_\mathrm{L} \\ v_\mathrm{c} \end{bmatrix} \tag{2.23}$$

• Mode 2: (Q1 is OFF, Q2 is OFF) :

For the duration (1/2-d)Ts, the equivalent circuit of the converter is as in Fig 2.6

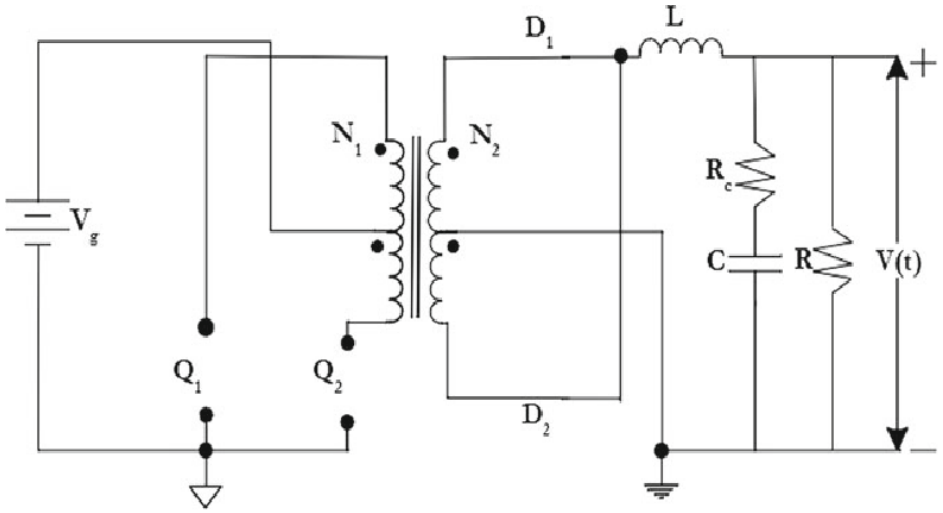

Figure 2.6: Equivalent circuit when Q1 and Q2 are OFF

$$V_{N_2} = 0 \tag{2.24}$$

$$V_L + V_R = 0 \tag{2.25}$$

$$V_L = -V_R \tag{2.26}$$

$$L\frac{dL}{dt} = -\frac{RR_c i_L}{R+R_c} - \frac{RV_c}{R+R_c} \tag{2.27}$$

$$\frac{cV_c}{dt} = \frac{Ri_L}{R+R_c} - \frac{V_c}{R+R_c} \tag{2.28}$$

$$V = \frac{RR_c iL}{R+R_c} + \frac{RV_c}{R+R_c} \tag{2.29}$$

The state equation and output equation are

$$\begin{bmatrix} L & 0 \\ 0 & C \end{bmatrix} \begin{bmatrix} \frac{\mathrm{d}i_\mathrm{L}}{\mathrm{d}t} \\ \frac{\mathrm{d}v_\mathrm{c}}{\mathrm{d}t} \end{bmatrix} = \begin{bmatrix} -\frac{RR_\mathrm{c}}{R+R_\mathrm{c}} & -\frac{R}{R+R_\mathrm{c}} \\ \frac{R}{R+R_\mathrm{c}} & -\frac{1}{R+R_\mathrm{c}} \end{bmatrix} \begin{bmatrix} i_\mathrm{L} \\ v_\mathrm{c} \end{bmatrix} \tag{2.30}$$

$$\begin{bmatrix} v \\ i_\mathrm{g} \end{bmatrix} = \begin{bmatrix} \frac{RR_\mathrm{c}}{R+R_\mathrm{C}} & \frac{R}{R+R_\mathrm{C}} \\ \frac{N_2}{N_1} & 0 \end{bmatrix} \begin{bmatrix} i_\mathrm{L} \\ v_\mathrm{c} \end{bmatrix} \tag{2.31}$$

Similar modeling can be arrived when switch Q2 is ON and Q1 is OFF. Thus, the ON and OFF period of the converter is 2dTs and (1/2-d)Ts, respectively. The average model of mode 1 and mode 2 can be written by using the equations. [31] [32]

Since mode 1 and 3 are the same we could write, The overall Matrix times the whole periode :

$$AT = 2dTA_1 + 2TA_2(\frac{1}{2} - d) \tag{2.32}$$

$$AT = 2dT(A_1 - A_2) + TA_2 \tag{2.33}$$

$$A = A_2 \tag{2.34}$$

$$BT = 2dTB_1 + 2TB_2(\frac{1}{2} - d) \tag{2.35}$$

$$BT = 2dT(B_1 - B_2) + TB_2 \tag{2.36}$$

$$B = 2d(B_1 - B_2) \tag{2.37}$$

$$CT = 2dTC_1 + 2TC_2(\frac{1}{2} - d) \tag{2.38}$$

$$CT = 2dT(C_1 - C_2) + TC_2 \tag{2.39}$$

$$C = C_1 = C_2 \tag{2.40}$$

$$ET = 2dTE_1 + 2TE_2(\frac{1}{2} - d) \tag{2.41}$$

$$ET = 2dT(E_1 - E_2) + TE_2 \tag{2.42}$$

$$E = 0 \tag{2.43}$$

Thus, the averaged model of the push–pull converter is:

$$A = \begin{bmatrix} -\frac{RR_c}{R+R_c} & -\frac{R}{R+R_c} \\ \frac{R}{R+R_c} & -\frac{1}{R+R_c} \end{bmatrix}, B = \begin{bmatrix} 2d\frac{N_2}{N_1} \\ 0 \end{bmatrix} \tag{2.44}$$

$$C = \begin{bmatrix} \frac{RR_c}{R+R_C} & \frac{R}{R+R_C} \\ \frac{N_2}{N_1} & 0 \end{bmatrix}, E = \begin{bmatrix} 0 \end{bmatrix} \tag{2.45}$$

For the above small signal models, the transfer functions output Current to input Current $G_{iVg}(s)$ is obtained as [31] [32]:

$$\begin{aligned} &\dot{x} = Ax + BU \\ &y = Cx + EU \\ &SX(S) - x(0) = AX(S) + BU(S) \\ &x(0) = 0 \\ &(\text{SI-A})X(S) = BU(S) \\ &X(S) = (SI - A)^{-1}BU(S) \\ &Y(S) = C(SI - A)^{-1}BU(S) \end{aligned} \tag{2.46}$$

$$\begin{aligned} &\frac{Y(S)}{U(S)} = C(SI - A)^{-1}B \\ &Y(S) = V(S) \quad ; U(S) = V_g(S) \\ &V(S) = RI(S) \Rightarrow \quad I(S) = \frac{1}{R}V(S) \\ &\frac{V(S)}{V_g(S)} = \frac{RI(S)}{V_g(S)} = C(SI - A)^{-1}B \\ &\Rightarrow \frac{I(S)}{V_g(S)} = \frac{1}{R}C(SI - A)^{-1}B \end{aligned} \tag{2.47}$$

$$\frac{I(S)}{V_g(S)} = \frac{2\ \mathrm{d}\frac{N_2}{N_1}\left(1 + sCR_C\right)}{s^2LC\left(R + R_C\right) + s\left(L + RR_CC\right) + R} \tag{2.48}$$

The transfer function output Current to duty $G_{id}(s)$ is obtained as :

$$\begin{aligned} \dot{x} &= Ax + fU \\ y &= Cx + EU \end{aligned} \tag{2.49}$$

$$\begin{aligned} &\frac{Y(S)}{U(S)} = C(SI - A)^{-1} f \\ &Y(S) = V(S) \quad ; U(S) = V_g(S) \\ &V(S) = RI(S) \Rightarrow \quad I(S) = \frac{1}{R} V(S) \\ &\frac{V(S)}{V_g(S)} = \frac{RI(S)}{V_g(S)} = C(SI - A)^{-1} f \\ &\Rightarrow \frac{I(S)}{Vg(S)} = \frac{1}{R} C(SI - A)^{-1} f \end{aligned} \tag{2.50}$$

Switch between the two modes mode 1 and mode 2 will be through d So:

when mode 1 ,w've f1=B1

when mode 2 ,w've f2=0

$$\begin{aligned} fT &= dTB_1 - Tf_2(\frac{1}{2} - d) \\ fT &= dT(f_1 - f_2) - Tf_2(\frac{1}{2}) \\ f &= B_1 d \end{aligned} \tag{2.51}$$

$$\begin{aligned} \frac{I(S)}{Vg(S)} &= \frac{1}{R} C(SI - A)^{-1} B1d \\ \frac{I(S)}{d(S)} &= \frac{1}{R} C(SI - A)^{-1} B1 v_g \end{aligned} \tag{2.52}$$

$$\frac{I(S)}{d(S)} = \frac{v_{\mathrm{g}} \frac{N_2}{N_1} (1 + SCR_{\mathrm{C}})}{S^2 LC (R + R_{\mathrm{C}}) + S (L + RR_{\mathrm{C}}C) + R} \tag{2.53}$$

2.5 Bode diagram

A Bode diagram is a graphical representation of the frequency response of a system. It consists of two plots: the magnitude plot and the phase plot. Bode diagrams are commonly used in control systems engineering and signal processing to analyze the behavior of a system in the frequency domain.

The magnitude plot displays the magnitude (in decibels) of the system's response as a function of frequency. It is typically plotted on a logarithmic scale, with frequency represented on the horizontal axis and magnitude on the vertical axis. The magnitude plot provides information about the amplification or attenuation of different frequencies by the system.

The phase plot displays the phase shift (in degrees) of the system's response as a function of frequency. Like the magnitude plot, the phase plot is also typically plotted on a logarithmic scale. It provides information about the phase delay introduced by the system at different frequencies.

Bode diagrams are useful for analyzing stability, gain margins, phase margins, and frequency response characteristics of a system. They can be generated either theoretically using mathematical equations or experimentally by measuring the system's response to different input signals at various frequencies.[33]

The Bode plot of output voltage to duty transfer function based on equation (equ 2.53) of open loop converter is shown in Fig 2.7, and the open loop Bode plot has a phase margin (PM) of 7.78db. To improve the performance parameters of the system, a PI compensator with transfer

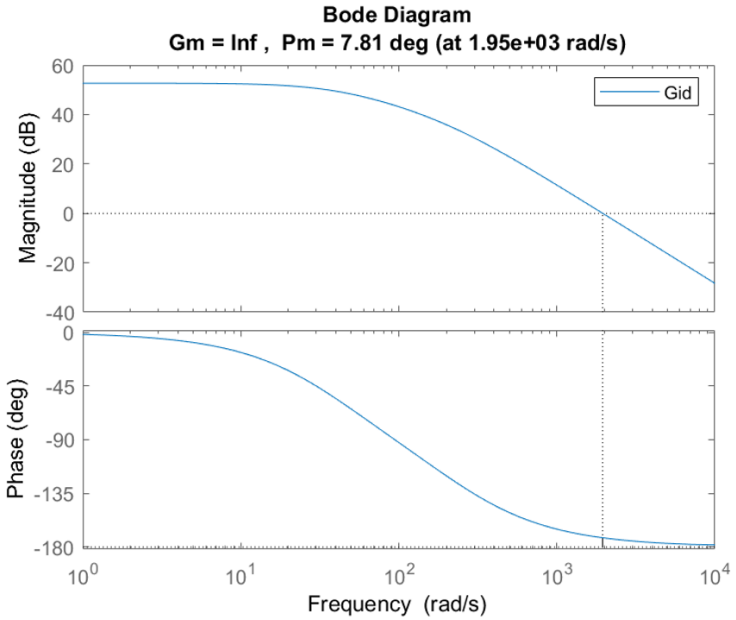

Figure 2.7: Open loop Bode plot of the converter

function as in Eq.(2.54) is added to the system:

$$F_{pi} = K_p + \frac{K_I}{S} \tag{2.54}$$

2.6 PI Controller

The controller is a power electronic system in which a specific parameter (output voltage, input current) must be controlled. This parameter is sensed and compared with a predetermined reference. The resulting error signal is given as follows Input to the controller that will generate a control parameter to obtain the desired output/response The factory is mostly controlled by service turn; Hence, it will be the voltage to time conversion to set the controller input to the output Required controller to meet the required performance of stability, speed and accuracy.[30]

PI controller is designed to have the following characteristics:

(1).A null steady-state error at the output of the converter.

(2). Large phase margin (79°) yielding well-damped transient load

responses to ensure good stability for sudden changes in the load and the output voltage.

The transfer function of push pull converter is given as :

$$\frac{I}{d} = \frac{K\left(1 + R_c C S\right)}{S^2 LC\left(R + R_c\right) + S\left(L + R R_c C\right) + R} \tag{2.55}$$

with: $L = 0.57\text{H}, R = 72\Omega, C = 1.6 \cdot 10^{-6}$ F

$$R_c = 0.1\Omega, K = \frac{N_2}{N_1} \times Vg$$

$$\frac{I}{d} = \frac{436\left(1 + S \cdot 1.6 \cdot 10^{-7}\right)}{\left(6.3 \cdot 10^{-5}\right) S^2 + 0.57S + 72}$$

$$\frac{I}{d} = \frac{436\left(1 + S \cdot 1.6 \cdot 10^{-7}\right)}{(S + 8641)(S + 128)}$$

when PI is added: $F_{pi} = K_p + \frac{K_I}{S}$

$$\Rightarrow Kp\left(\frac{\frac{1}{T} + S}{S}\right) \text{ and } T = \frac{K_p}{K_I}$$

$$G_s = \frac{436\left(1 + S \cdot 1.6 \cdot 10^{-7}\right)}{(s + 8641)(S + 128)} \times \frac{K_p\left(S + \frac{1}{T}\right)}{S}$$

when $S + \frac{1}{T} = S + 128 \Rightarrow \frac{1}{T} = 128$

$$\Rightarrow T = \frac{1}{128} = 7.8 \times 10^{-3}$$

$$G_s = \frac{k_p 436\left(1 + S \cdot 1.6 \cdot 10^{-7}\right)}{(S + 8641)S}$$

$$G_s(j\omega) = \frac{k_p 436\left(1 + j\omega 1.6 \cdot 10^{-7}\right)}{-\omega^2 + j\omega 8641}$$

$$|G_s(j\omega)| = \frac{k_p 436\sqrt{1 + (\omega \cdot 1.6 \cdot 10^{-7})^2}}{\sqrt{\omega^4 + (8641\omega)^2}}$$

$$M_G = 20\log\left(k_p 436\right) + 10\log\left(1 + \left(\omega 1.6 \cdot 10^{-7}\right)^2\right) - 10\log\left(\omega^4 + (8641\omega)^2\right)$$

for $t_r = 10$ ms we have : At frequency 100 Hz

$$M_G = -108\text{db}$$

we find a value

$$Kp = 7.8 \cdot 10^{-3}$$

so: $T = \frac{Kp}{K_I} \Rightarrow K_I = \frac{Kp}{T} = 1$

$$K_p = 7.8 \cdot 10^{-3} \text{ and } K_I = 1$$

respectively. The bode plot of The Closed Loop transfer Function.

2.7 Simulation, Results and Observations

Due to addition of the compensator, the system has a gain margin of 34 db and phase margin of 79.4 db at a frequency of 6.37 Hz as shown in figure 2.8 .

The step response obtained from the system shown in Fig 2.9 has a settling time of 10ms.

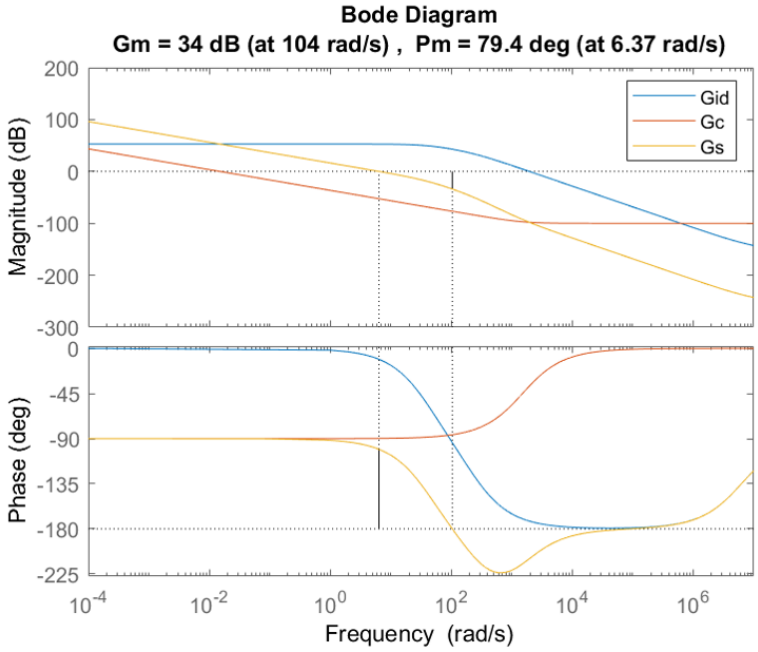

Figure 2.8: Bode plot of the closed loop system

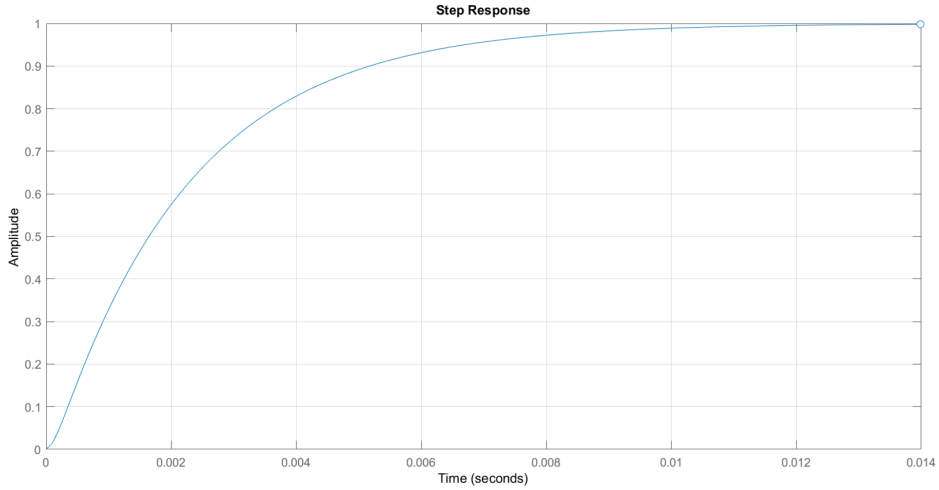

Figure 2.9: Step response of closed loop system

Simulink model of the push-pull converter with the design parameters is shown in Fig 2.10.

From the figure 2.11 one can see the effectiveness of PI controller in point of view response time against the sudden variation of the set point.

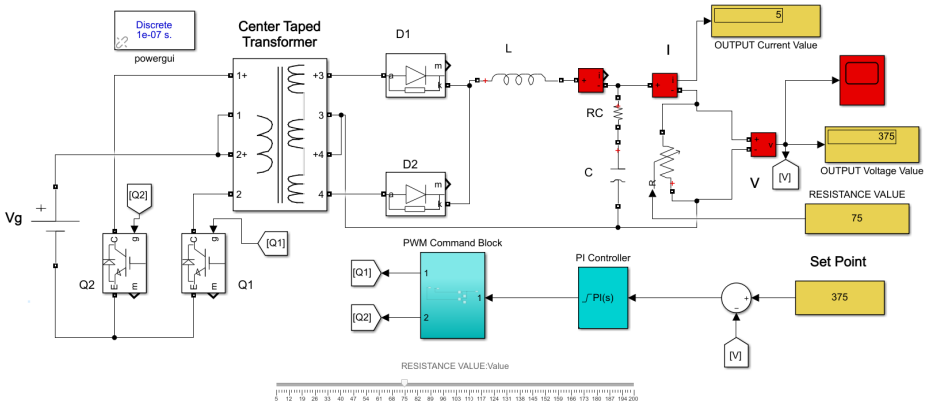

Figure 2.10: Simulink model of push pull converter

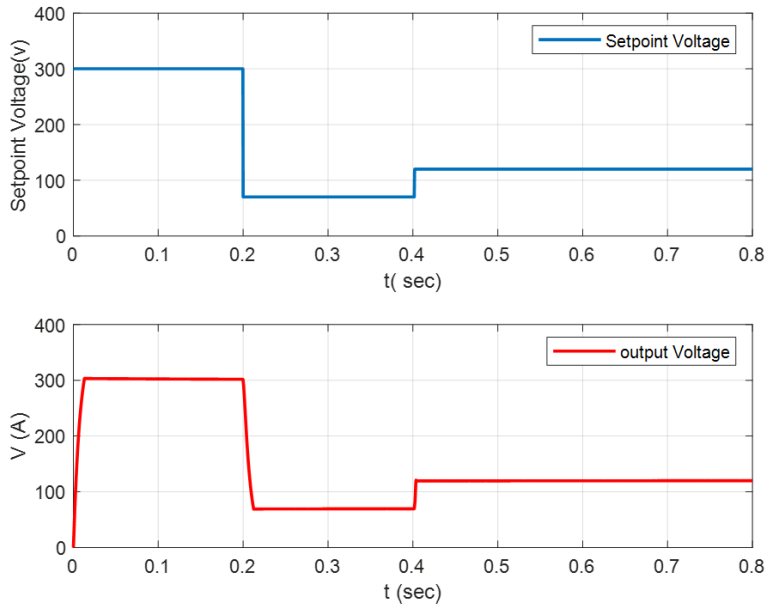

Figure 2.11: Signal build response of the closed loop system

2.8 Conclusion

In this chapter a 1.2 kW, 36-375 V push–pull converter is modeled using state space average technique. The inclusion of PI controller makes the converter stable and improves the settling time of the controller. The designed converter response is verified in MATLAB Simulink.

Chapter 3

Simulation And Validation Of PV emulator

3.1 Introduction

A PV emulator is a programmable DC source which has similar electrical characteristics to a PV panel but it is not affected by external factors such as temperature and illumination. In this chapter a photovoltaic emulator will be designed and simulated under Matlab/Simulink environment with multiple tests of irradiance, temperature and load .

3.2 Functional description of the PVE

A Push-Pull converter has been chosen as a PV emulator due to the following reasons:

- High Efficiency.
- Galvanic Isolation.
- Wide Input Voltage Range.
- Low Output Ripple.
- Step-up or step-down Operation.

Perhaps the most important component of a solar PV emulator is its mathematical model since the accuracy of the emulated characteristics

purely depends on this model. The closed loop control strategy is shown in Figure 3.1, it is used to control the duty cycle of the DC-DC push-pull converter switch. The mathematical model serving as reference provides the panel reference current , this current is compared with the push-pull converter feedback current , and the error e generated is fed to the controller [34].

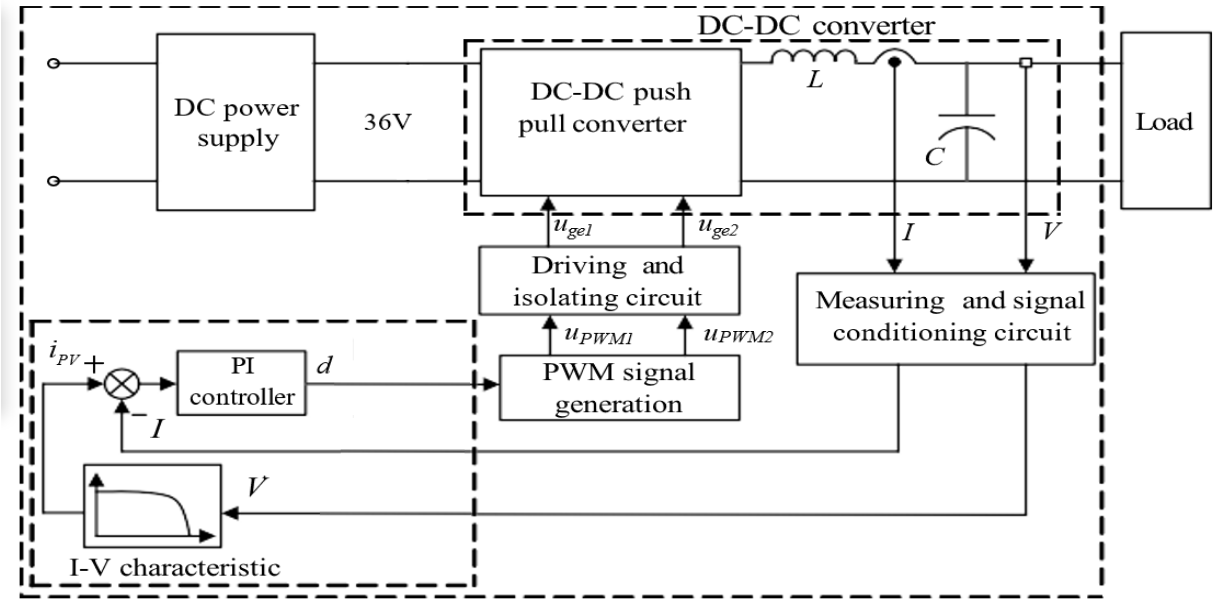

Figure 3.1: PV Emulator Block Diagram.

3.2.1 Mathematical model of PV array

It is necessary to know the basic properties of a PV system to perform emulation. Also, it is necessary to know specific characteristics of modules a PV system is made up of [35]. based on the simplified model that mentioned in the first chapter, Section 1.6.2, for this work the simulated mathematical PV model is based on it.

For our work we based on two real panels, Zergoun ZGE-FM72-385 panel and Solar world SW 85 poly R5A/D panel, their electricals con-

struction parameters are given in the following tables:

- Zergoun ZGE-FM72-385 Panel parameters :

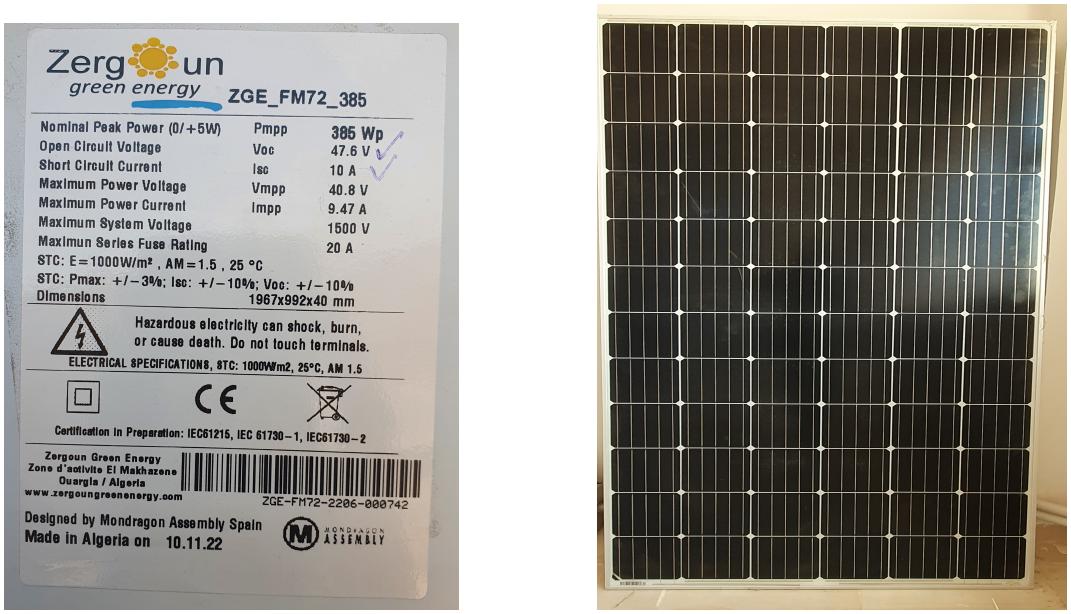

(a) (b)

Figure 3.2: (a). PV panel parameter, (b). Real PV Module of Zergoun ZGE-FM72-385

maximum power (Pmax)	385 W
Voltage at maximum power (VMP)	40.8 V
current at maximum power (IMP)	9.47 A
Open circuit voltage (Voc)	47.6 V
Short circuit current (Isc)	10 A

Table 3.1: Specification of the Zergoun panel parameters.

- Solar World SW 85 poly R5A/D panel parameters :

(a) (b)

Figure 3.3: (a). PV Panel parameter, (b). Solar world SW 85 poly R5A/D

maximum power (Pmax)	85 W
Voltage at maximum power (VMP)	17.9 V
current at maximum power (IMP)	4.77 A
Open circuit voltage (Voc)	22 V
Short circuit current (Isc)	5.20 A

Table 3.2: Specification of Solar World panel parameters.

3.2.2 GPV characteristics of zergoun ZGE-FM72-385 panel

Figure 3.4 shows the I-V and P-V curves of the PV module zergoun ZGE-FM72-385 panel simulated in MATLAB SIMULINK at STC. [8]

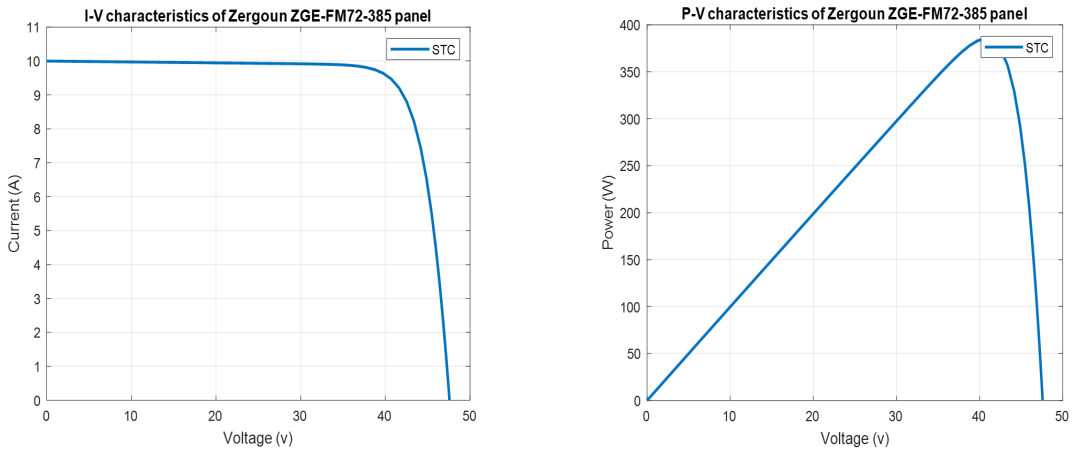

Figure 3.4: I-V and P-V curves of Zergoun ZGE-FM72-385

3.2.3 GPV characteristics of Solar world SW 85 poly R5A/D panel

Figure 3.5 shows the I-V and P-V curves of the PV module Solar world SW 85 poly R5A/D simulated in MATLAB at STC.

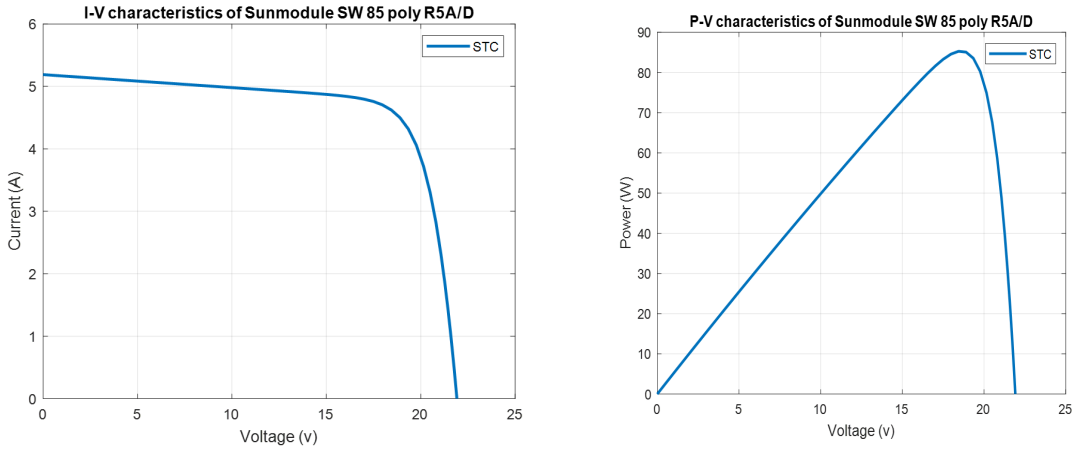

Figure 3.5: I-V and P-V curves of Solar world SW 85 poly R5A/D

3.2.4 Temperature and irradiance effects

The output power of a PV panel changes in accordance with changes in solar radiation and temperature levels. [9] For different levels of solar radiation, the short circuit current varies in proportion to the level of solar radiation, while the open circuit voltage is approximately constant. The effect of temperature on PV characteristics is less compared to that of solar radiation, the current increases slightly as the temperature increases, which is due to the increased absorption of light. However, as the temperature increases the open circuit voltage tends to decrease. These changes in weather conditions are shown by the I-V and the P-V curves of zergoun PV Panel displayed in Figures 3.8 and 3.9 and sunmodule PV panel in Figures 3.10 and 3.11 .

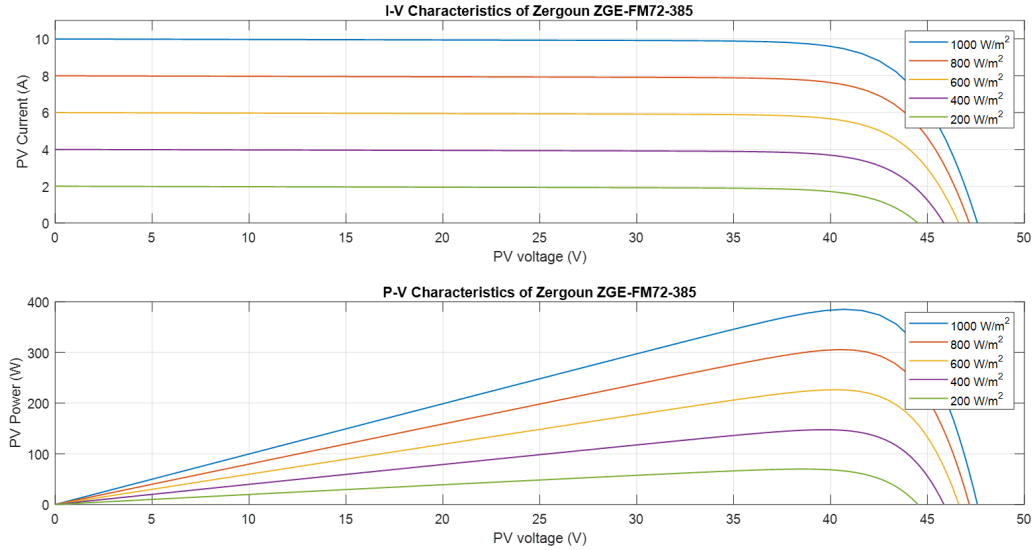

Figure 3.6: I-V and P-V curves under radiation effects.

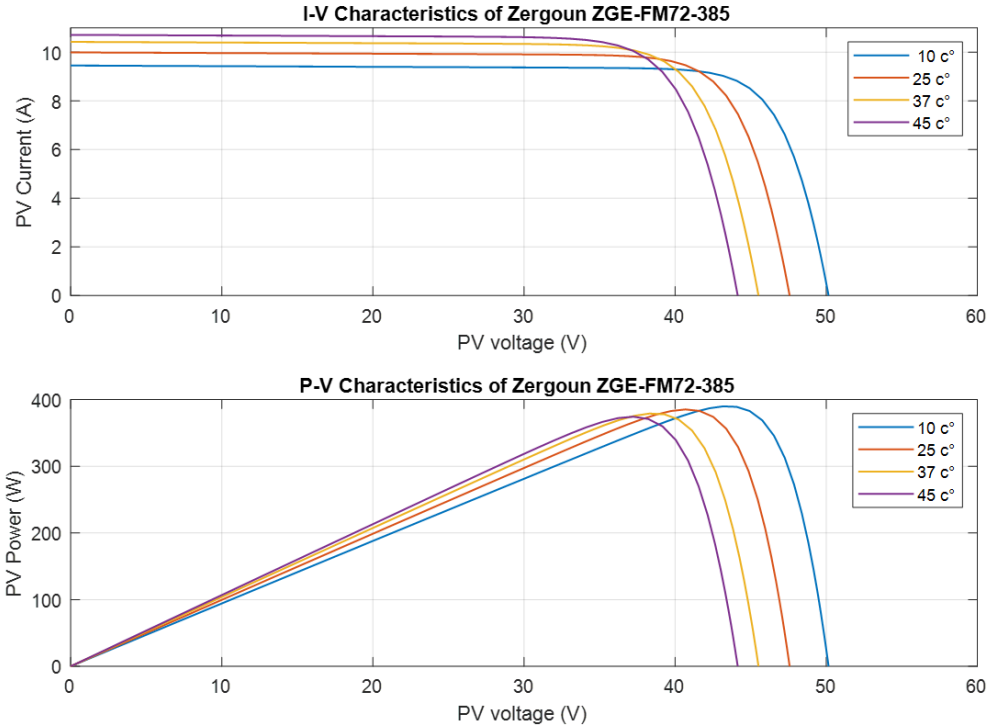

Figure 3.7: I-V and P-V curves under Temperature effects.

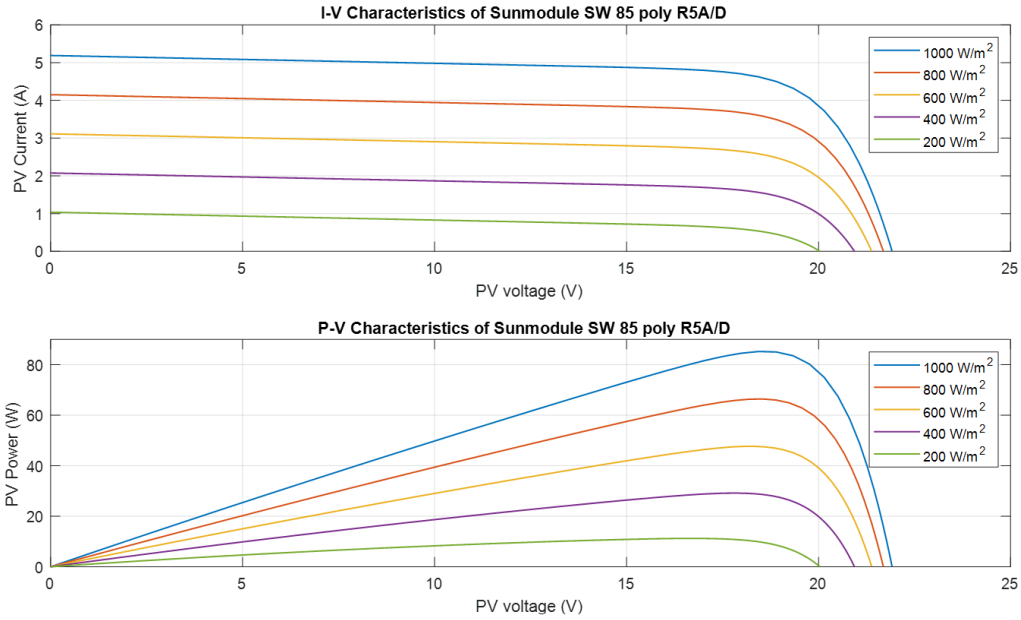

Figure 3.8: I-V and P-V curves under radiation effects.

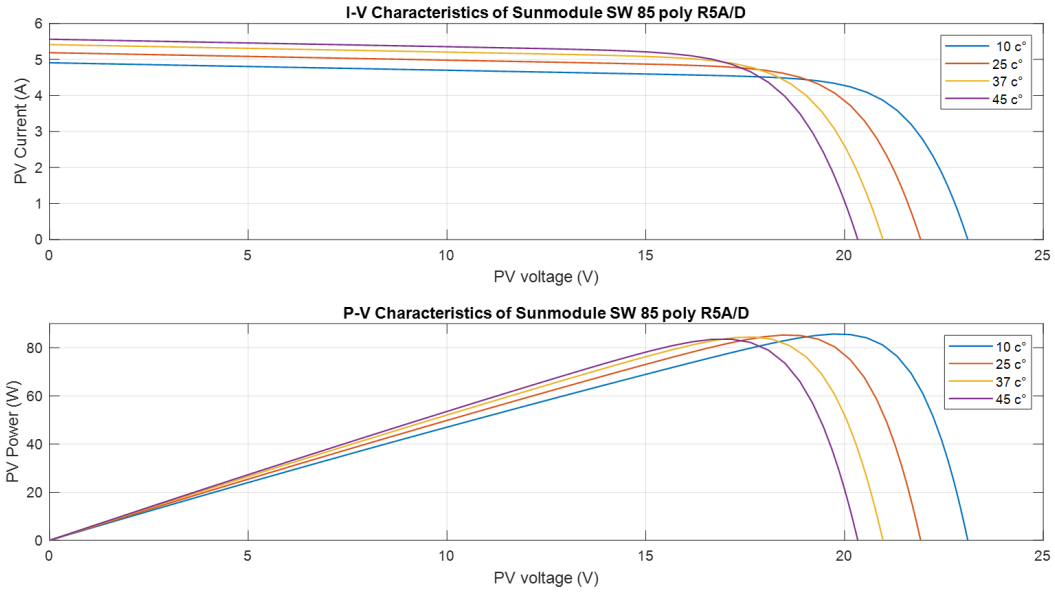

Figure 3.9: I-V and P-V curves under Temperature effects.

3.3 Simulation of the PV Emulator Performance

In this section, we present simulation of PV model with mathematical equations and proposed PV Emulator. The proposed PV emulator tested under multiple tests of irradiance, temperature and load with abrupt scenario in order to test the robustness of our proposed PV emulator. The mathematical PV model and PV emulator are modeled and simulated in MATLAB/SIMULINK as shown in Figures 3.10 and 3.11 respectively.

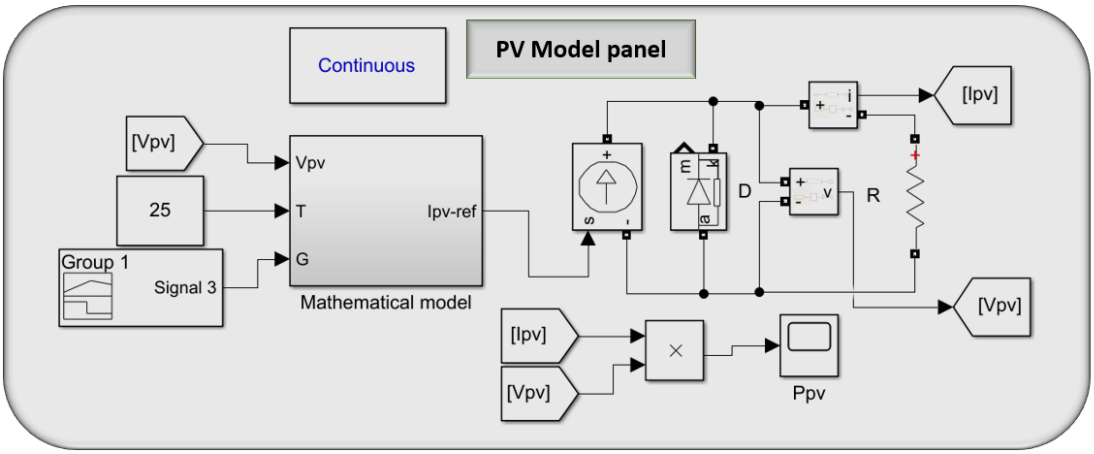

Figure 3.10: PV model simulation diagram in MATLAB/ SIMULINK.

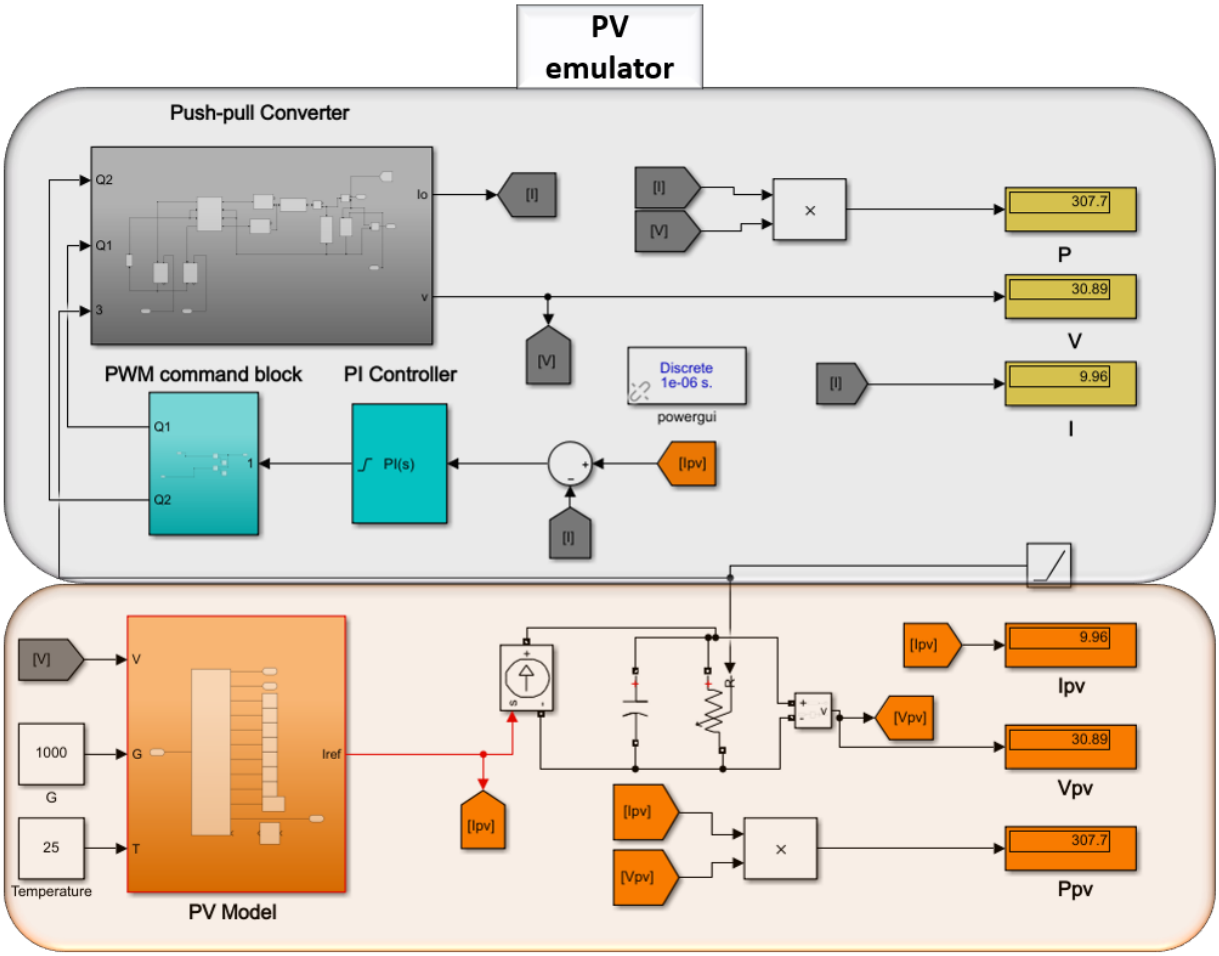

Figure 3.11: PV emulator simulation diagram in MATLAB/ SIMULINK.

3.3.1 PV emulator under sudden changes of Irradiance

The PV emulator is tested for MPP condition by connecting the load resistance of value equal to the internal impedance at MPP of the PV panel. At this value of load resistance, PV model is delivering the 385W power which is the maximum power of the zergoun panel at standard test condition (STC). For the same load, PV emulator set the reference current value to 9.47A, which is regulated through the load and thus the PV emulator is delivering the voltage 40.8V and the power of 385W corresponding to MPP at STC as shown in Figure 3.12.

And the same operation is applied to sunmodule panel, The PV em-

ulator is tested for MPP condition by connecting the load resistance of value equal to the internal impedance at MPP of the PV panel. At this value of load resistance, PV model is delivering the 85W power which is the maximum power of the Sunmodule panel at standard test condition (STC). For the same load, PV emulator set the reference current value to 4.77A, which is regulated through the load and thus the PV emulator is delivering the voltage 17.9V and the power of 85W corresponding to MPP at STC as shown in Figure 3.13.

At fixed load of 4.31 Ω , PV emulator and PV mathematical model are tested by changing the irradiance from 1000 W/m^2 to 700 W/m^2 at t=0.2s and from 700 W/m^2 to 900 W/m^2 at t=0.4s as shown in figure 3.1. The performance indicated in Figure 3.14 A, concludes that the emulator characteristics are matching with the mathematical modeling of PV cell characteristics. This confirms that the proposed algorithm is working effectively.

The exact same scenario was applied to the Solar World SW 85 poly R5A/D panel at a fixed load of 3.75Ω, as shown if figure 3.13.

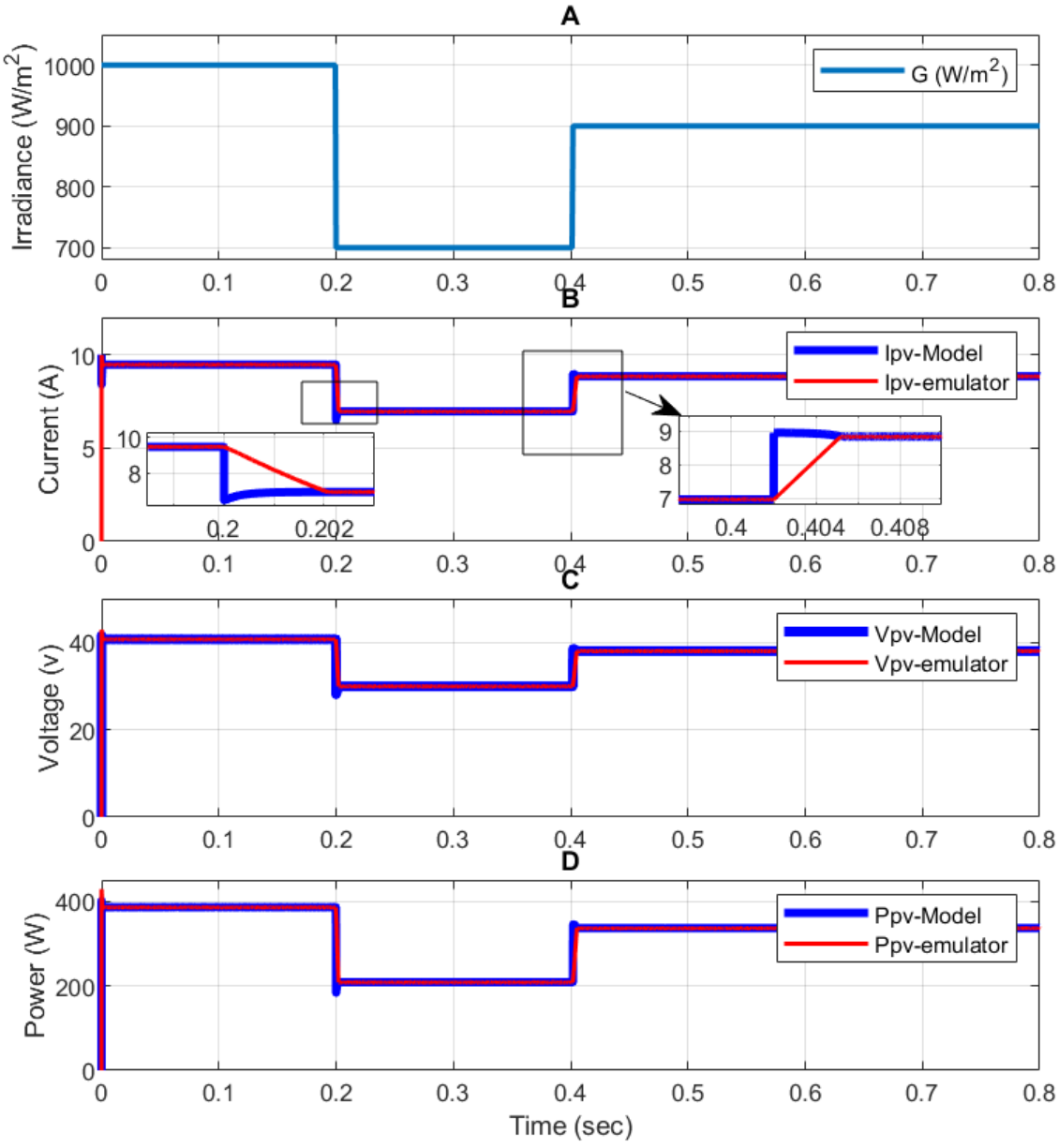

Figure 3.12: PV emulator of Zergoun panel under Irradiance effect in MATLAB SIMULINK.

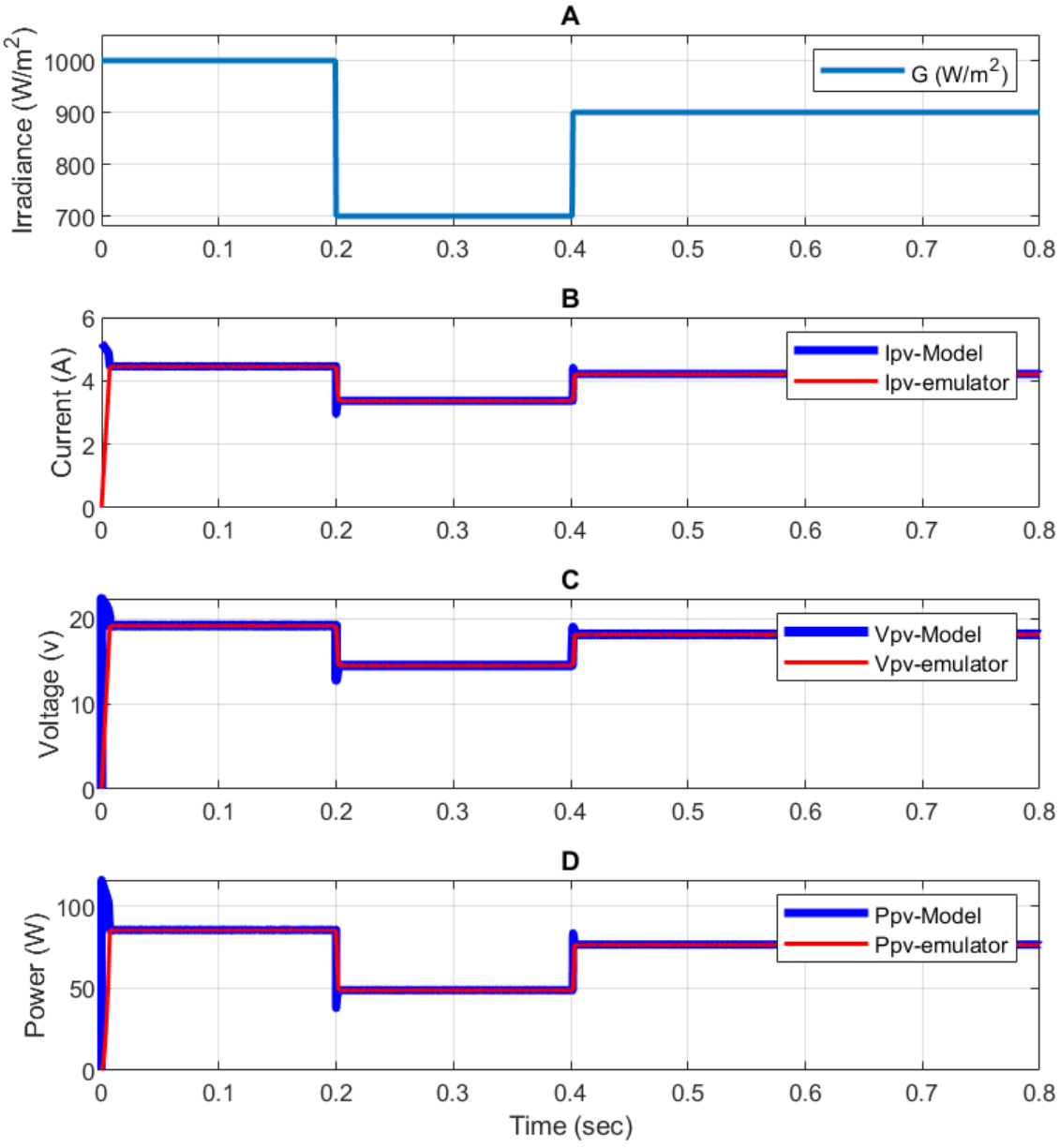

Figure 3.13: PV emulator of Sunmodule panel under Irradiance effect in MATLAB SIMULINK.

3.3.2 PV emulator under sudden changes of Temperature

In the next section at fixed load of 4.3 Ω for zergoun panel and 3.75 Ω for Solar World panel , PV emulator and PV mathematical model are tested by changing the Temperature from 25 C° to 10 C° at t=0.2s and from 10 C° to 40 C° at t=0.4s as shown in figure 3.14.(A) The performance indicated in Figures 3.14 and 3.15 concludes that the emulator characteristics are matching with the mathematical modeling of PV cell characteristics. This confirms that the proposed Emulator is working effectively.

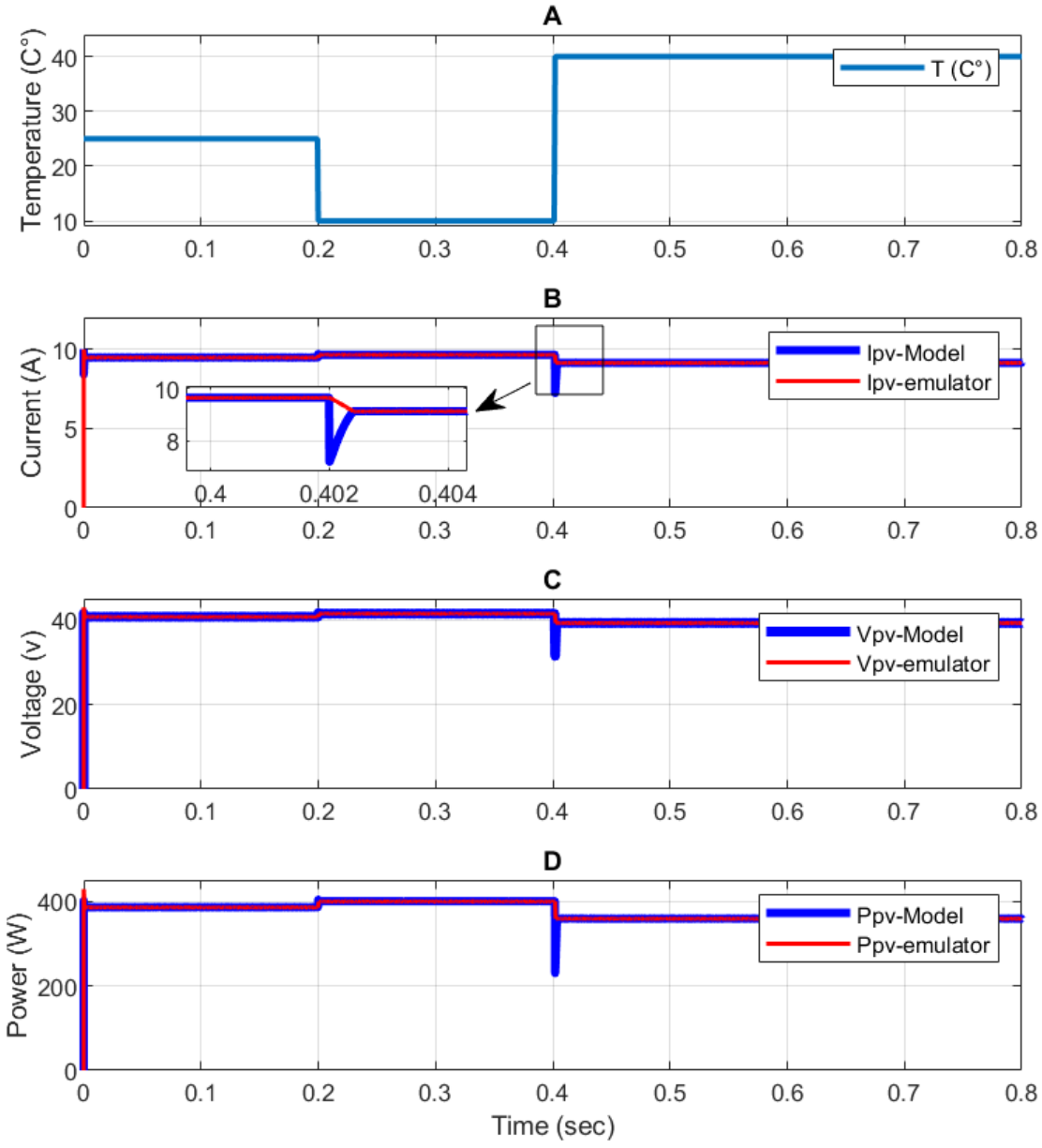

Figure 3.14: PV emulator of Zergoun panel under Temperature effect in MATLAB SIMULINK.

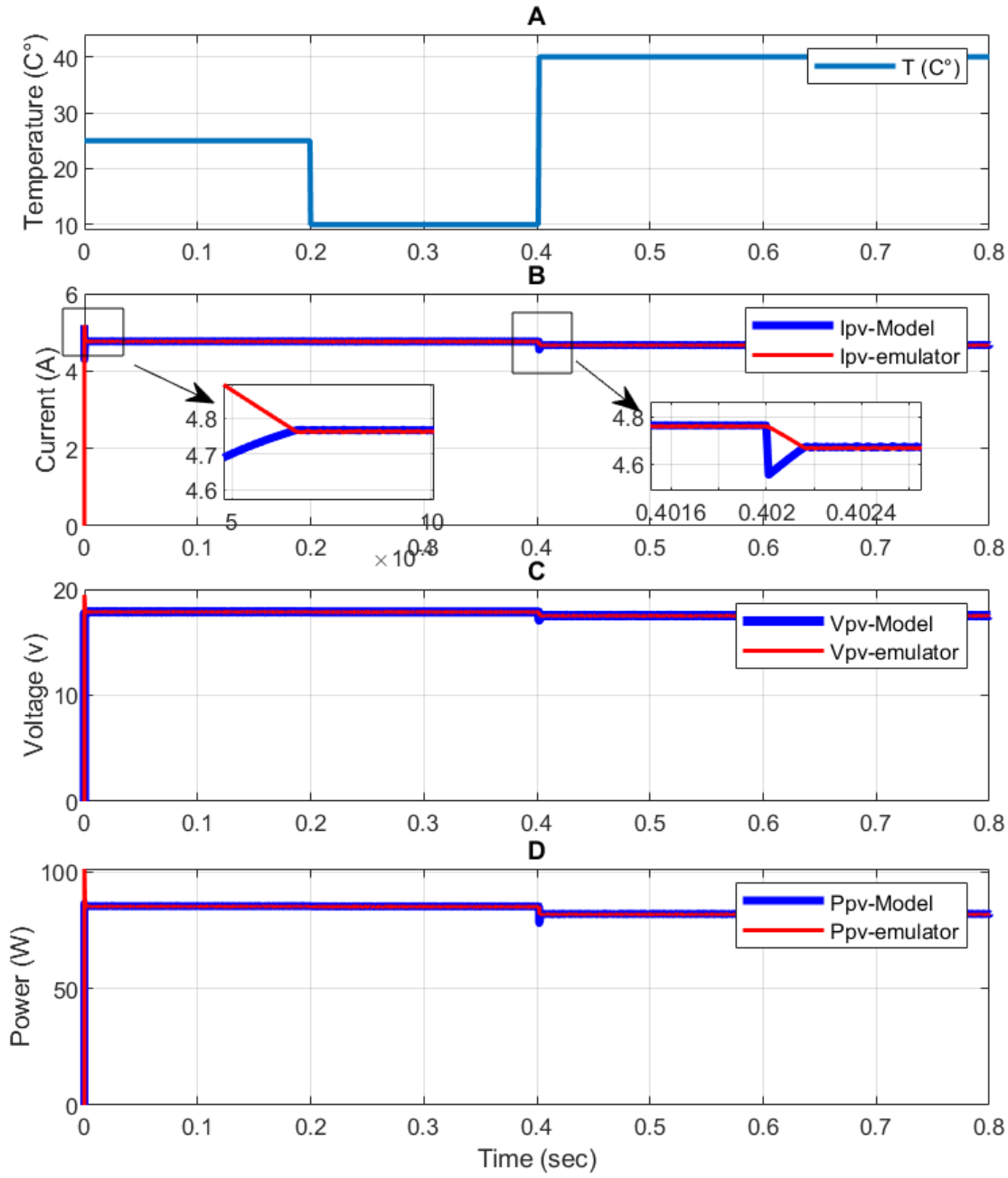

Figure 3.15: PV emulator of Sunmodule panel under Temperature effect in MATLAB SIMULINK.

3.3.3 PV emulator under Load variation

The next section represent the PV emulator compared to Pv model panel under load variation, we used Ramp signal in MATLAB SIMULINK. in this way we included all the load points as shown in figures 3.16 and 3.17.

The performance indicates that the emulator characteristics are matching with the mathematical modeling of PV panel characteristics at STC, This confirms that the proposed emulator is working effectively.

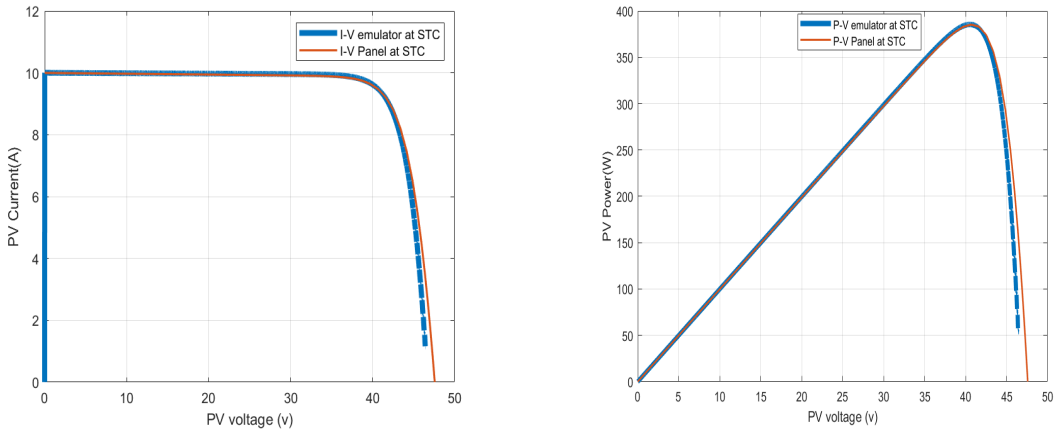

Figure 3.16: I-V and P-V curves of Zergoun ZGE-FM72-385

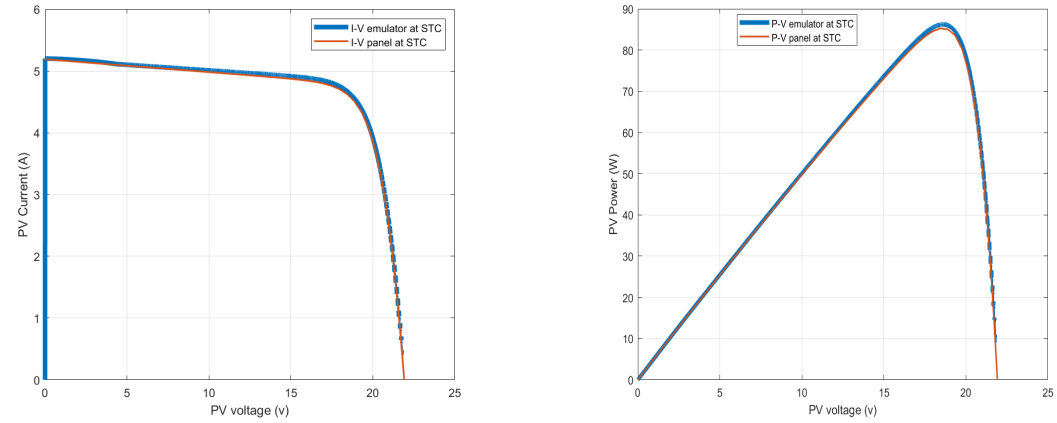

Figure 3.17: I-V and P-V curves of Solar World SW 85 poly R5A/D

3.4 Conclusion

In this chapter, a solar PV emulator using a DC-DC push pull converter controlled via a PI controller emulating solar PV characteristics is simulated. The simulated solar PV emulator is interfaced to the push pull converter. Various performance tests were conducted on the proposed setup to examine dynamic behavior, rapidity, and viability of the system. Based on simulation and the proposed emulator is fast and accurate solar PV emulator with easy and simple real-time control, also it has a fast dynamic response and highly stable output. Further, the system is also capable of emulating any operating point of the solar PV curve by changing the solar cell parameters.

General Conclusion

In this study, we focused on the development, modeling, and simulation of a photovoltaic emulator based on a push-pull converter. In the first chapter, we provided comprehensive definitions and background information on photovoltaic emulators and DC-DC converters, establishing a solid foundation for our research. In the second chapter, we delved into the modeling and control aspects of the push-pull converter, ensuring a thorough understanding of its behavior and operation.

Through extensive simulations and validations presented in the third chapter, we demonstrated the effectiveness and accuracy of our PV emulator. The results obtained were highly satisfactory, confirming the successful implementation of our proposed system. The PV emulator showed excellent performance in emulating the behavior of a real photovoltaic system, allowing for reliable and efficient testing of various power electronics applications and control strategies.

Overall, this research contributes to the field of photovoltaic emulation and provides valuable insights into the modeling and control of push-pull converters. The developed PV emulator presents a robust and accurate tool for experimental investigations, enabling researchers and engineers to explore and optimize the performance of power electronics systems connected to photovoltaic sources. Further research can focus

on expanding the scope of applications and exploring additional control strategies to enhance the versatility and functionality of the PV emulator.

Bibliography

[1] Seif El Islam Remache and Kamel Barra. Performance comparison among boost and multi level boost converters for photovoltaic grid connected system using finite set model predictive control. In 2018 9th international renewable energy congress (IREC), pages 1–6. IEEE, 2018.

[2] John Lee. Basic calculation of a buck converter's power stage. Application Note AN041, Richtek Technology Corporation, pages 1–8, 2015.

[3] Razman Ayop and Chee Wei Tan. A comprehensive review on photovoltaic emulator. Renewable and Sustainable Energy Reviews, 80:430–452, 2017.

[4] Younghyun Kim, Woojoo Lee, Massoud Pedram, and Naehyuck Chang. Dual-mode power regulator for photovoltaic module emulation. Applied energy, 101:730–739, 2013.

[5] Yuan Li, Taewon Lee, Fang Z Peng, and Dichen Liu. A hybrid control strategy for photovoltaic simulator. In 2009 Twenty-Fourth Annual IEEE Applied Power Electronics Conference and Exposition, pages 899–903. IEEE, 2009.

[6] Tuan Dat Mai, Sven De Breucker, Kris Baert, and Johan Driesen. Reconfigurable emulator for photovoltaic modules under static partial shading conditions. Solar Energy, 141:256–265, 2017.

[7] Qingrong Zeng, Pinggang Song, and Liuchen Chang. A photovoltaic simulator based on dc chopper. In IEEE CCECE2002. Canadian Conference on Electrical and Computer Engineering. Conference Proceedings (Cat. No. 02CH37373), volume 1, pages 257–261. IEEE, 2002.

[8] Chouki Balakishan and BABU Sandeep. Development of a microcontroller based pv emulator with current controlled dc/dc buck converter. International journal of renewable energy research, 4(4):1049–1055, 2014.

[9] Dale Dolan, Joseph Durago, Joe Crowfoot, et al. Simulation of a photovoltaic emulator. In North American Power Symposium 2010, pages 1–7. IEEE, 2010.

[10] Khiem Nguyen-Duy, Arnold Knott, and Michael AE Andersen. High dynamic performance nonlinear source emulator. IEEE Transactions on Power Electronics, 31(3):2562–2574, 2015.

[11] Maria Carmela Di Piazza and Gianpaolo Vitale. Photovoltaic sources: modeling and emulation. Springer, 2013.

[12] Ankur V Rana and Hiren H Patel. Current controlled buck converter based photovoltaic emulator. Journal of Industrial and Intelligent Information Vol, 1(2), 2013.

[13] MC Di Piazza, M Pucci, A Ragusa, and G Vitale. A grid-connected system based on a real time pv emulator: design and experimental

set-up. In IECON 2010-36th Annual Conference on IEEE Industrial Electronics Society, pages 3237–3243. IEEE, 2010.

[14] A Vijayakumari, AT Devarajan, and N Devarajan. Design and development of a model-based hardware simulator for photovoltaic array. International Journal of Electrical Power & Energy Systems, 43(1):40–46, 2012.

[15] Massimo Merenda, Demetrio Iero, Riccardo Carotenuto, and Francesco G Della Corte. Simple and low-cost photovoltaic module emulator. Electronics, 8(12):1445, 2019.

[16] Vun Jack Chin, Zainal Salam, and Kashif Ishaque. Cell modelling and model parameters estimation techniques for photovoltaic simulator application: A review. Applied Energy, 154:500–519, 2015.

[17] Kun Ding, XinGao Bian, HaiHao Liu, and Tao Peng. A matlab-simulink-based pv module model and its application under conditions of nonuniform irradiance. IEEE Transactions on Energy Conversion, 27(4):864–872, 2012.

[18] Widalys De Soto, Sanford A Klein, and William A Beckman. Improvement and validation of a model for photovoltaic array performance. Solar energy, 80(1):78–88, 2006.

[19] Djamila Rekioua and Ernest Matagne. Optimization of photovoltaic power systems: modelization, simulation and control. Springer Science & Business Media, 2012.

[20] Hayrettin Can, Damla Ickilli, and Koray Sener Parlak. A new numerical solution approach for the real-time modeling of photovoltaic panels. In 2012 Asia-Pacific Power and Energy Engineering Conference, pages 1–4. IEEE, 2012.

[21] Chris Deline, Bill Sekulic, Josh Stein, Stephen Barkaszi, Jeff Yang, and Seth Kahn. Evaluation of maxim module-integrated electronics at the doe regional test centers. In 2014 IEEE 40th Photovoltaic Specialist Conference (PVSC), pages 0986–0991. IEEE, 2014.

[22] Nor Hanisah Baharudin, TMNT Mansur, Fairuz Abdul Hamid, Rosnazri Ali, and Muhammad Irwanto Misrun. Topologies of dc-dc converter in solar pv applications. Indonesian Journal of Electrical Engineering and Computer Science, 8(2):368–374, 2017.

[23] Yavuz Koç, Yaşar Birbir, and Hacı Bodur. Non-isolated high step-up dc/dc converters–an overview. Alexandria Engineering Journal, 61(2):1091–1132, 2022.

[24] AJ Forsyth and SV Mollov. Modelling and control of dc-dc converters. Power engineering journal, 12(5):229–236, 1998.

[25] J Blahins, A Bziskjan, A Apsitis, A Ubelis, and Anatoly Kravtsov. Journal home page: http://www. journalijiar. com. Journal home page: http://www. journalijiar. com, 5(9).

[26] Andrea Stratta, Davide Gottardo, Mauro di Nardo, Liliana de Lillo, Lee Empringham, Jordi Espina, and Mark Johnson. Automated design of integrated inductive components for dc-dc converters. In 2021 IEEE Design Methodologies Conference (DMC), pages 1–6. IEEE, 2021.

[27] Jeba Singh Oliver, Prince Winston David, Praveen Kumar Balachandran, and Lucian Mihet-Popa. Analysis of grid-interactive pv-fed bldc pump using optimized mppt in dc–dc converters. Sustainability, 14(12):7205, 2022.

[28] John D Prymak. New tantalum capacitors in power supply applications. In Conference Record of 1998 IEEE Industry Applications Conference. Thirty-Third IAS Annual Meeting (Cat. No. 98CH36242), volume 2, pages 1129–1137. IEEE, 1998.

[29] Yi Liu, Meng Huang, Huai Wang, Xiaoming Zha, Jinwu Gong, and Jianjun Sun. Reliability-oriented optimization of the lc filter in a buck dc-dc converter. IEEE Transactions on Power Electronics, 32(8):6323–6337, 2016.

[30] L Umanand. Power Electronics: Essentials and Applications. Wiley India Pvt. Limited, 2009.

[31] Domingos Sávio Lyrio Simonetti, JLF Viera, and Gilberto Costa Drumond Sousa. Modeling of the high-power-factor discontinuous boost rectifiers. IEEE transactions on industrial electronics, 46(4):788–795, 1999.

[32] Robert W Erickson and Dragan Maksimovic. Fundamentals of power electronics. Springer Science & Business Media, 2007.

[33] Katsuhiko Ogata et al. Modern control engineering, volume 5. Prentice hall Upper Saddle River, NJ, 2010.

[34] Mohammed Azharuddin, Thanikanti Sudhakar Babu, Nishant Bilakanti, and Natarajan Rajasekar. A nearly accurate solar photovoltaic emulator using a dspace controller for real-time control. Electric Power Components and Systems, 44(7):774–782, 2016.

[35] Denis Pelin, Jelena Jukić Antolović, and Vjekoslav Rapčan. Pv emulator. International journal of electrical and computer engineering systems, 5(1.):21–26, 2014.